



LABORATÓRIO NACIONAL
DE ENGENHARIA CIVIL

DEPARTAMENTO DE HIDRÁULICA E AMBIENTE
Núcleo de Águas Subterrâneas
UNIVERSIDAD DE CHILE, FACULTAD DE CIENCIAS
Departamento de Ciencias Ecológicas
Laboratorio de Modelación Ecológica

Proc. 0607/17/15488

ECOMANAGE

Integrated Ecological Coastal Zone Management System

Deliverables 2.6 & 2.8 – CHILE

D2.6 – SIG mapping of hydrogeologic parameters, including groundwater recharge assessment and vulnerability to pollution

D2.8 – Groundwater flow and transport components of the global estuary model

Study developed for the European Commission
DG Research INCO-CT Programme under contract
number INCO-CT-2004-003715

Study developed within the framework of LNEC Research
Plan for 2005-2008, referring to the study "Optimised
management of coastal aquifers and interaction between
ground and surface waters"

Lisboa • Dezembro de 2006

I&D HIDRÁULICA E AMBIENTE

RELATÓRIO 379/2006 – NAS

DELIVERABLES 2.6 & 2.8 - CHILE
D2.6 - SIG MAPPING OF HYDROGEOLOGIC PARAMETERS, INCLUDING GROUNDWATER
RECHARGE ASSESSMENT AND VULNERABILITY TO POLLUTION
D2.8 - GROUNDWATER FLOW AND TRANSPORT COMPONENTS OF THE GLOBAL ESTUARY
MODEL

ABSTRACT

Current knowledge about the geology, soils, climate, and fluviometric regimes in the Aysén basin is presented. The surface flow hydrograph separation method is applied in two watersheds within the basin in conjunction with a snowmelt model. This model is based on simplified energy balance equations and was implemented in Microsoft Excel. The results show that groundwater recharge is relatively high in both watersheds and that snowmelt can be the major component of streamflow during the spring months. Differences, especially in the magnitude of the flow rates, were observed between the two study watersheds, underlining the heterogeneity of the Aysén basin as a whole.

A brief analysis of the applicability of the DRASTIC index in the Aysén basin is presented. It is concluded that the index could be applied to the area between the towns of Coyahique and Balmaceda. However, a general lack of good-quality information on the hydrogeology of the region undermines the confidence that we can place in the results of indices or models.

DELIVERABLES 2.6 & 2.8 - CHILE

D2.6 – MAPEAMENTO SIG DE PARÂMETROS HIDROGEOLÓGICOS, INCLUINDO A CARACTERIZAÇÃO DA RECARGA DAS ÁGUAS SUBTERRÂNEAS E DA VULNERABILIDADE À POLUIÇÃO

D2.8 – AS COMPONENTES DE FLUXO E DE TRANSPORTE DE ÁGUAS SUBTERRÂNEAS DO MODELO GLOBAL DO ESTUÁRIO

RESUMO

Apresenta-se informação relevante sobre o sistema físico da bacia do rio Aysén, incluindo informação sobre a geologia, solos, clima, e regimes fluviais. Aplica-se o método da decomposição do hidrograma de escoamento superficial a duas sub-bacias hidrográficas associado a um modelo simples de acumulação de neve e de derretimento de neve. Este modelo baseia-se em equações simplificadas do balanço de energia e foi implementado em Microsoft Excel. Os resultados mostram que a recarga de águas subterrâneas é relativamente alta em ambas as sub-bacias e que o derretimento de neve pode ser uma componente importante dos caudais dos rios nos meses da Primavera. Foram observadas diferenças especialmente de caudais entre as duas sub-bacias, sublinhando a heterogeneidade da bacia de Aysén.

Faz-se uma análise breve sobre a aplicação possível do índice DRASTIC na bacia do rio Aysén. Conclui-se que o índice poderia ser aplicado à área situada entre as cidades de Coyahique e Balmaceda. Contudo, a inexistência de informação de boa qualidade acerca da hidrogeologia da região induz muita incerteza associada aos índices e modelos usados na bacia.

DELIVERABLES 2.6 & 2.8 - CHILE

D2.6 - MAPEO SIG DE PARAMETROS HIDROGEOLOGICOS, INCLUYENDO LA EVALUACION DE RECARGA DE AGUAS SUBTERRANEAS Y LA VULNERABILIDAD A LA CONTAMINACION

D2.8 – COMPONENTES DE FLUJO Y TRANSPORTE DE AGUAS SUBTERRANEAS DEL MODELO ESTUARINO GLOBAL

RESUMEN

Se presenta información relevante sobre el sistema físico de la cuenca del Río Aysén, incluyendo información sobre clima, suelos, geología, y regímenes fluviales. El método de separación de hidrógrafa está aplicado a dos subcuencas junto con un modelo simple de acumulación y derretimiento de nieve. Este modelo está basado en ecuaciones simplificadas de balance de energía y fue implementado en Microsoft Excel. Los resultados muestran que la recarga de aguas subterráneas es relativamente alta en ambas subcuencas y que el derretimiento de nieve puede ser un componente importante de los caudales de los ríos en los meses de primavera. Diferencias entre las cuencas fueron observadas, especialmente en cuanto a los caudales, subrayando la idea de la cuenca de Aysén como una cuenca muy heterogénea en muchos aspectos.

Un análisis breve de la posible aplicación de la índice DRASTIC in la cuenca de Aysén es presentado. Se concluye que la índice podría ser aplicado en el sector entre Balmaceda y Coyhaique. Sin embargo, una ausencia generalizada sobre la hidrogeología de la región significa que existe mucha incertidumbre asociada con las índices y los modelos usados en la cuenca.

ACKNOWLEDGEMENTS

Juan Salas and Francisco Riestra of the DGA – XI Region of Chile, Paola Almeida and Dr. Rossella Napolitana of the University of Trieste, Fernando Escobar Caceres of the DGA – Santiago, Dr. Victor Marín of the University of Chile, and a MESECUP travel grant for graduate students.

TABLE OF CONTENTS

1 Introduction	1
2 General Description	2
2.1 Location	2
2.2 Topography	2
2.3 Geology	4
2.4 Pedology	5
2.5 Climate	6
2.6 Fluviometric regimes	8
3 Estimation of groundwater recharge	9
3.1 Introduction	9
3.2 Surface flow hydrograph separation method	11
3.3 Simple energy-budget snowmelt model	14
3.4 Incorporating snowmelt in the hydrograph separation method	21
3.5 Results of snowmelt and hydrograph separation models	21
3.5.1 Rio Claro Watershed	21
3.5.2 Coyhaique Watershed	25
4 Groundwater vulnerability to pollution	28
4.1 Concept of vulnerability to pollution	28
4.2 Methods for vulnerability assessment	28
4.3 The DRASTIC method	29
4.3.1 General description	29
4.3.2 Depth to the water (D)	31
4.3.3 Net Recharge (R)	32
4.3.4 Aquifer media (A)	32
4.3.5 Soil media (S)	33
4.3.6 Topography (T)	34
4.3.7 Impact of the vadose zone media (I)	34
4.3.8 Hydraulic Conductivity of the aquifer (C)	35
4.4 Potential for the application of the DRASTIC method in Aysén	36
4.4.1 Depth to the water (D)	36
4.4.2 Net Recharge (R)	36
4.4.3 Aquifer media (A)	36
4.4.4 Soil media (S)	36
4.4.5 Topography (T)	37
4.4.6 Impact of the vadose zone media (I)	37
4.4.7 Hydraulic Conductivity of the aquifer (C)	37
5 Conclusions	38
6 Bibliography	40

FIGURES

Fig. 1 – The Aysén Fjord and river basin. The main range of the Southern Andes corresponds to the area of finally dissected terrain running north to south. [Map generated from the digital elevation model (DEM), SERPLAC].....	2
Fig. 2 – Major watersheds contributing to the Aysén Fjord	3
Fig. 3 – Geology of the Aysén Basin (Source: Servicio Nacional de Geología y Minería (2004) – Mapa Geológico de Chile: Versión Digital, Escala 1:1,000,000).....	4
Fig. 4 – Soil map of the Aysén Basin, based on the IREN-CORFO study of 1979.....	6
Fig. 5 – Weather stations and Isohyets (mm/yr) in the Aysén basin.....	7
Fig. 6 – Fluvimetry of the Rio Aysen: probability of exceedence	8
Fig. 7 – Fluvimetry of the Rio Simpson: probability of exceedence	9
Fig. 8 – Method to separate total flow in direct runoff and base flow.....	12
Fig. 9 – Example of the process of hydrograph separation, for $n = 2$ day, using as criterion (A) the day of the hydrograph peak, (B) the last precipitation day.....	12
Fig. 10 – Schematic representation of main processes related to snowmelt.....	14
Fig. 11 – Equations used in snowmelt model.....	16
Fig. 12 – Flow chart for Snowmelt model.....	18
Fig. 13 – Snow cover winter – summer 2005- 2006. From MODIS imagery.	19
Fig. 14 – Modeled snowpack, Coyhaique watershed. Three vertical bands are shown; values are in mm of water equivalent.....	20
Fig. 15 – Modeled snowpack, Rio Claro watershed. Three vertical bands are shown; values are in mm of water equivalent.....	20
Fig. 16 – Hydrograph separation with snowmelt	21
Fig. 17 – Hydrograph separation detail, Rio Claro watershed. The streamflow and precipitation (rain + snowmelt) are represented in units of mm/day. The shaded areas represent baseflow discharge, while the solid colors represent surface runoff.....	23
Fig. 18 – Hydrograph separation without snowmelt, Rio Claro watershed. The streamflow and precipitation (only rain) are represented in units of mm/day. The shaded areas represent baseflow discharge, while the solid colors represent surface runoff.	23
Fig. 19 – Probability distribution function of baseflow for Rio Claro watershed. This figure is based on data from the period: December 2003 – August 2005.	25
Fig. 20 – Probability distribution function of baseflow for Coyhaique watershed. This figure is based on data from the period: January 2000 – February 2003.....	27
Fig. 21 - Parameters of the DRASTIC method	30

TABLES

Table 1 – Major watersheds contributing to the Aysén Fjord. The watersheds that are part of the Aysén Basin are in bold.	3
Table 2 – Climatic information for three towns within the Aysén Basin. They occur along the pronounced West – East gradient of climatic conditions occurring within the basin.	7
Table 3 – Weighting factors for structural vegetation classes	15
Table 4 – Weighting factors for structural vegetation classes	16
Table 5 – Source of parameters and variables used in snowmelt model	17
Table 6 – Snowmelt model zones based on elevation and annual precipitation. The percent forest cover within each zone is indicated in parentheses.....	22
Table 7 – Monthly values for baseflow and associated variables, Rio Claro watershed.	24
Table 8 – Monthly values for baseflow and associated variables, Coyhaique watershed	26
Table 9 - Assigned weights for DRASTIC features used in Standard and Pesticide DRASTIC	31
Table 10 - Ranges and ratings for D - Depth to water.....	32
Table 11 - Ranges and ratings for R - net Recharge.....	32
Table 12 - Ranges and ratings for A - Aquifer media	33
Table 13 - Ranges and ratings for S - Soil media.....	34
Table 14 - Ranges and ratings for T – Topography.....	34
Table 15 - Ranges and ratings for I - Impact of the vadose zone media	35
Table 16 - Ranges and ratings for C - Hydraulic conductivity	36

DELIVERABLES 2.6 & 2.8 - CHILE

D2.6 - SIG MAPPING OF HYDROGEOLOGIC PARAMETERS, INCLUDING GROUNDWATER RECHARGE ASSESSMENT AND VULNERABILITY TO POLLUTION

D2.8 - GROUNDWATER FLOW AND TRANSPORT COMPONENTS OF THE GLOBAL ESTUARY MODEL

1 Introduction

A primary objective of the ECOManage project is to assist managers of coastal zones through the creation of tools that allow an exploration of different development or management scenarios. ECOManage is based conceptually on the DPSIR assessment framework (Driving forces, Pressures, State, Impacts, and Responses). It is recognized that the watersheds adjacent to coastal zones contribute to the physical and ecological dynamics and therefore must be considered. In other words, the pressures of largely terrestrial activities in contributing watersheds can affect coastal areas through transport of nutrients or pollutants via rivers or groundwater. In this sense, a goal of ECOManage is to understand hydrological pathways that lead from contribution terrestrial areas to the coastal systems under study. In this deliverable, available information is analyzed in order to understand hydrogeological dynamics and processes and vulnerabilities to contamination.

The Aysén Fjord is one of the three PHES-systems being analyzed and modelled under ECOManage. The fjord receives freshwater mainly from the Aysén river watershed ($Q > 700 \text{ m}^3\text{s}^{-1}$) (ECOManage deliverable 1.4). It is important to note that more than 89% of the population of the XI region of Chile lives in the Aysén basin, so the main anthropogenic pressures are centred here. Previous deliverables (1.4) have examined vegetation cover and landscape pattern and their potential influence on water quality. Here the hydrogeology of the basin is examined. First, groundwater recharge is analyzed using the hydrograph separation method. Because of the higher latitude and mountainous terrain of the Aysén Basin, it is important to consider the impact of snowfall and snowmelt on hydrographs and on groundwater recharge.

2 General Description

2.1 Location

The area of study is located in the XI administrative region of Chile (between 45°S and 46°S). ECOManage is concerned primarily with the Aysén Fjord and considers the dynamics of the contributing watersheds. The Aysén River Basin is the principal watershed having a total surface area of 11,674 km². The Aysén Fjord and Aysén Basin can be seen in **Fig. 1**. **Fig. 2** and **Table 1** list the principal watersheds. Information on the geology and aquifers in the Aysén region is limited and due to practical concerns this deliverable looks primarily at the hydrogeology of the area to the East of the main Andes range, in the upper Rio Simpson valley.

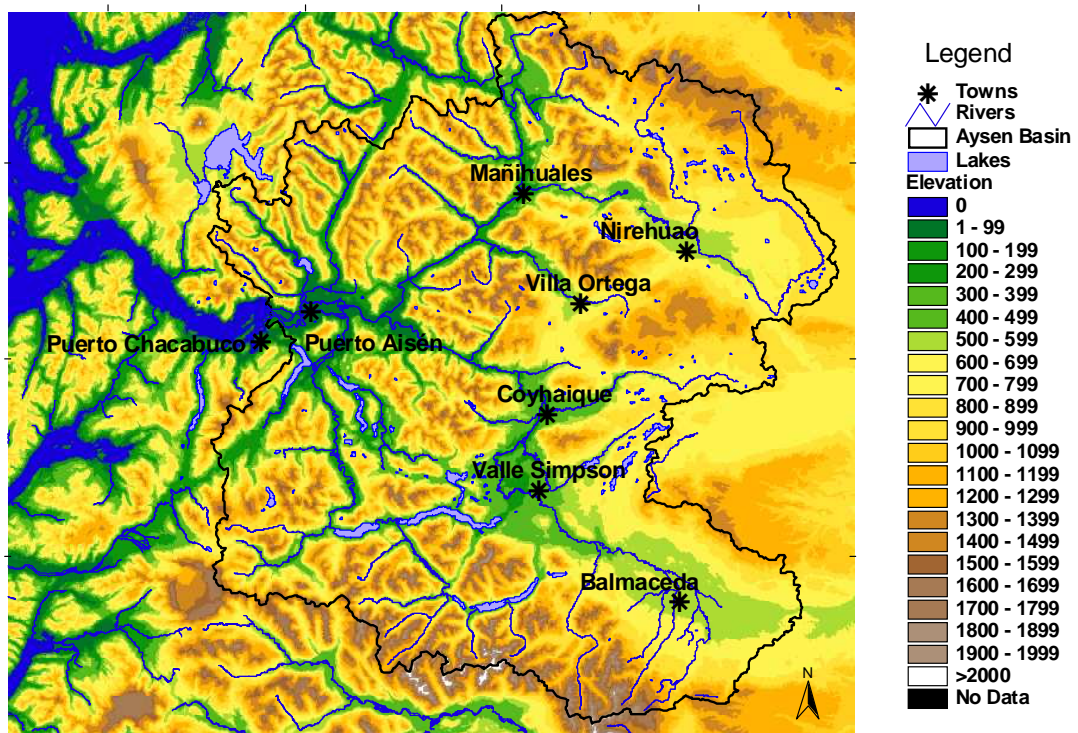


Fig. 1 – The Aysén Fjord and river basin. The main range of the Southern Andes corresponds to the area of finally dissected terrain running north to south. [Map generated from the digital elevation model (DEM), SERPLAC]

2.2 Topography

Topography may be understood by consulting **Fig. 1**. The Southern Andes have experienced a subsidence over geologic time and several periods of intense glaciation (CADE-IDEPE 2004). This can be seen in the relatively low altitudes (maximum elevation is 2227 m) and steep slopes. Furthermore, the intense pluviometric regimes on the Western slope of the Andes chain represent a powerful driver for erosion and have augmented the dissected topography of the area. Several large lakes of glacial

origin are located in the Andean range, Southeast of the Aysén Fjord. Montgomery *et al.* (2001) suggest that large scale climate patterns represent a first-order control on the topography of the Southern Andes. They hypothesize that removal of material by glacial and fluvial processes at higher latitudes have limited the elevation of the Southern Andes.

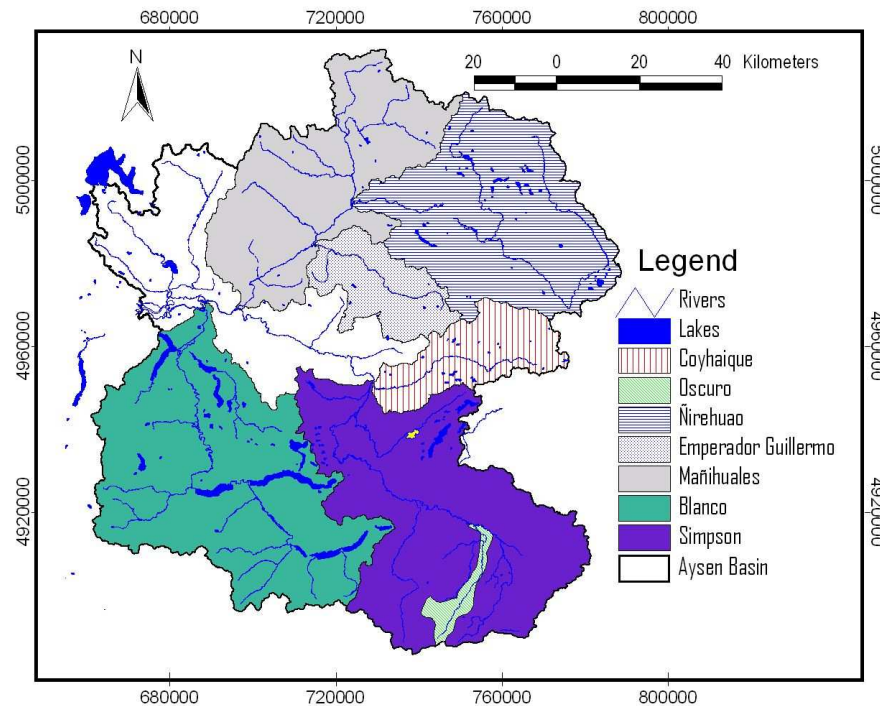


Fig. 2 – Major watersheds contributing to the Aysén Fjord

Table 1 – Major watersheds contributing to the Aysén Fjord. The watersheds that are part of the Aysén Basin are in bold.

Watershed/ Basin	Area (km ²)	Average Streamflow (m ³ s ⁻¹)	Annual Precipitation (mmyr ⁻¹)
Aysén Basin below confluence with Rio Los Palos	11674 ^a	543.7 ^c	>4000mm (Western border), <300mm (Eastern border) ^d
Rio Simpson below confluence with Rio Coyhaique	3712 ^a	49.3 ^c	1500mm (confluence with R. Mañihuales) to <300mm (Eastern edge) ^d
Rio Coyhaique	621 ^b	6.5 ^c	1385mm (Coyhaique pluviometric station) to <300mm (Eastern edge)
Rio Oscuro	106 ^b	2.1 ^c	600mm - 800mm ^d
Rio Ñirehuao	1910 ^b	33.4 ^c	1500 (confluence with R. Mañihuales), <300 (East) ^d
Rio Emperador Guillermo	651 ^b	18 ^c	2000mm - 1000mm ^d
Rio Mañihuales	3821 ^b	156.9 ^c	3000mm (near outlet) to <300m (Eastern edge) ^d
Rio Blanco ^a	3034	99.7	3520
Rio Condor ^a	460	46.4	5260
Rio Cuervo ^a	699	108.8	6270

Sources: (a) CEA 2005. (b) CADE-IDEPE 2004. (c) DGA 2005 (d) GIS files, SERPLAC

The Eastern part of the Aysén Basin lies on the Eastern slopes of the Andes and the transition to a plateau of 700 to 1000m along the Argentine border. Glacial processes have fragmented the Southern Andes at this latitude allowing water to drain to the Pacific from the east side of the range. Here the average slope, as calculated from the digital elevation model of the Aysén Basin, drops to 8% from 23% in the main Andean range. The eastern slope of the Andes experiences less pluviometric erosion but eolic erosion can be important along the border with Argentina.

2.3 Geology

The Aysén basin is located northeast of the Chile Triple Junction, a point of convergence between the South American plate, the Nazca plate, and the Antarctic plate. The subduction zone along the Western edge of the South American plate gives rise to a volcanic arc, of which several volcanoes (outside of the Aysén basin proper) have greatly influenced the geology and soils of the Aysén basin. It is worth mentioning the Macá Volcano near the headwaters of the Cuervo River and the Hudson Volcano on the southwest border of the Aysén basin. The Hudson has been recently active, with three eruptions in the last 40 years (Gutierrez *et al.* 2005). A prominent tectonic feature of the Southern Andes is an 1100 km long strike-slip fault zone: the Lliquiñe-Ofqui Fault Zone. It is part of the larger Southern Andean Volcanic Zone (SVZ). The materials originating from volcanic activity in the SVZ are typically calc-alkaline and are linked to the subduction of the Nazca Plate (Gutierrez *et al.* 2005). It is important to note that while subduction off the South American Plate has probably been occurring since the Jurassic, the building of the modern Andes has taken place in the last 15-25 Ma (Rosenau 2004).

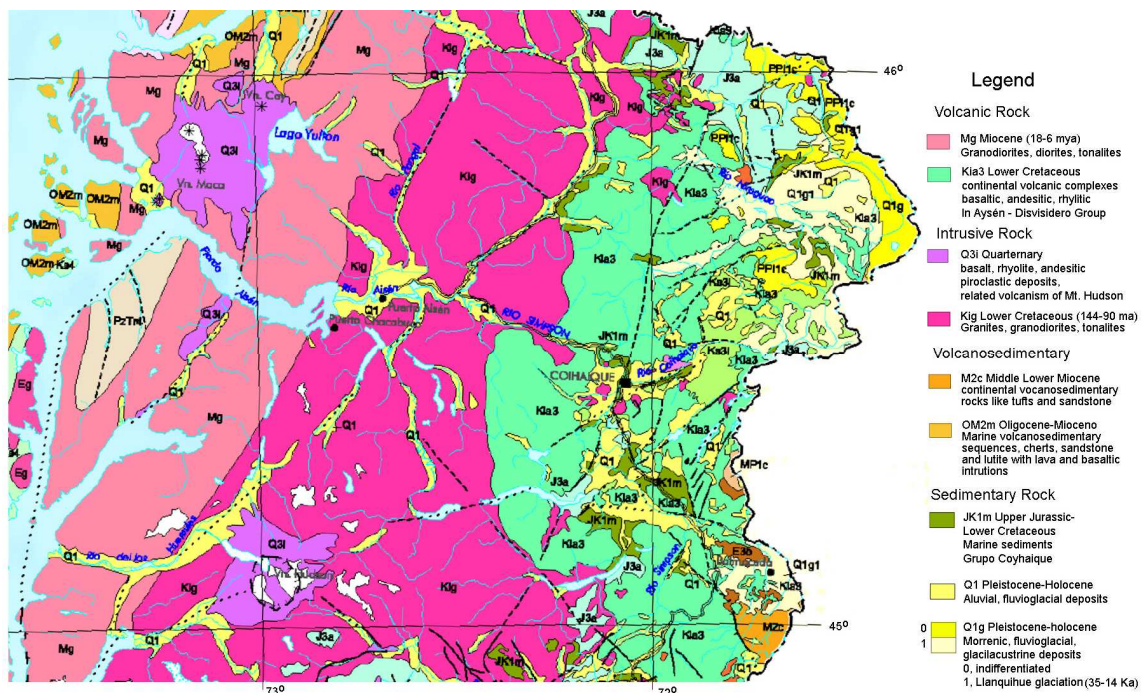


Fig. 3 – Geology of the Aysén Basin (Source: Servicio Nacional de Geología y Minería (2004) – Mapa Geológico de Chile: Versión Digital, Escala 1:1,000,000)

From the Geologic Map of Chile, a 1:1000000 scale map of the country, it is possible to establish the general geological patterns for the Aysén basin (**Fig. 3**). On the Western slope of the Andean range, passing just to the west of Puerto Aysén and including the Cuervo and Condor watersheds, is series from the Miocene (18-6Ma) typical of the North Patagonian batholith and made up principally of intrusive rocks such as granodiorites, diorites and tonalites. A similar series from the Lower Cretaceous (144-90 Ma) is composed of granite, granodiorite, tonalites of hornblende y biotite. To the East of this formation is volcanic sequence from the Lower Cretaceous that generally corresponds to the Divisidero group made up of intercalastic lava that vary from andesites to rhyolites. Along the principal fluvial systems, there are more recent alluvial and fluvialglacial deposits from the Holocene and Pleistocene.

The most recent and detailed geologic map corresponds to the area along the Argentine border between the towns of Coyhaique and Balmaceda. It includes the geologically complex Valle Simpson, an area of interest for ECOManage because of intensive cattle ranching land-use.

2.4 Pedology

Due to climate and often infertile or poorly developed soils, agriculture is limited to 1,607 hectares in the Aysén basin, or about 0.1% of the land surface (CADE-IDEPE 2004). As a result, there exists only one complete soil description of the Aysén basin from 1979 (IREN-CORFO). However, this work is essentially descriptive and many important edaphic parameters have therefore not been quantified in a comprehensive way. Nevertheless, several patterns are clear. First, the soils of the Aysén basin are generally young, having developed after the last glacial event (the Llanquihue event from 33.5 to 13.9 Ka). In addition, the erosion and mass wasting processes that occur in the Andes Mountains also mean that many forest soils are thin and undeveloped. In addition, the intentional burning of large tracts of forest in the decade of the 1940s has lead to major erosion of certain soils. As can be seen in the map in **Fig. 4**, the majority of soils as classified by textural class have a high percentage of sand. Some minor areas, where low velocity fluvial deposits (such as the area near the outlet of the Aysén river), have finer textures. Other areas associated with wetlands or small lakes have hydric soils, in some instances organic (peat) soils. The 'mountain soils' indicated in **Fig. 4** are a large heterogeneous group of soils that tend to be prone to erosion or landslides. The organic material content can be quite high, above 20% in most cases (Silva et al. 1999). Although there is little description of the soils occurring above the tree line, it is known that they are very thin and covered with snow for long periods every year. This class also includes glaciers.

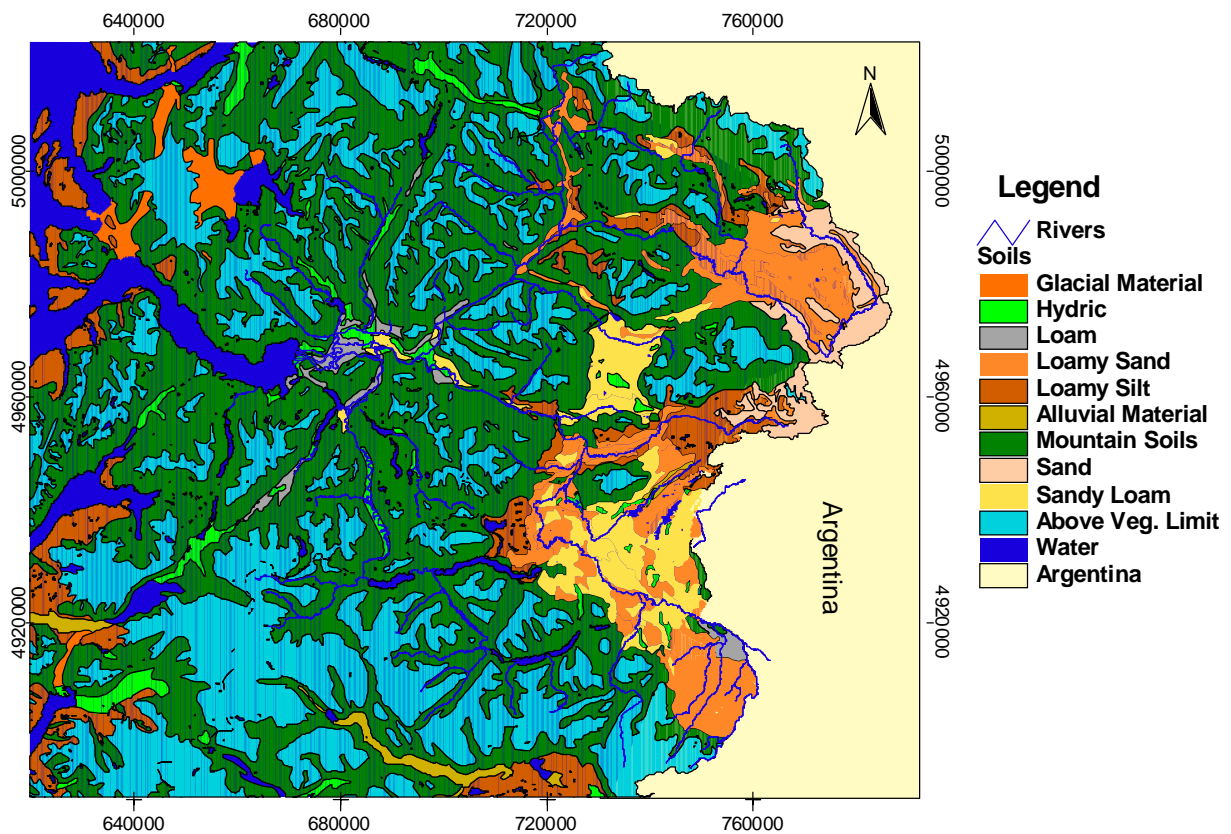


Fig. 4 – Soil map of the Aysén Basin, based on the IREN-CORFO study of 1979

2.5 Climate

The climate of the Aysén basin is spatially quite varied and precipitation and temperature gradients are often pronounced within the basin. Low pressure anticyclones in the Southern Pacific draw a great deal of moisture to the Southern Chilean Coast. In the cold oceanic climates of the fjords, rain is plentiful all year, often reaching annual values of 4000 mm. The influence of the ocean moderates temperatures and snowfall is limited to higher elevations in the coastal mountains. Puerto Aysén is located in this area of cold oceanic climate. In the Andes proper, the annual precipitation begins decrease, although humidity remains high year-round. In this area, of which the city of Coyhaique might be considered part, the annual temperature becomes lower with greater daily and seasonal temperature oscillations. Along the Argentine border, the mean annual temperature drops further, although the number of cloudy days is considerable lower. The number of windy days increases notable and wind can significantly influence patterns of vegetation and soil erosion. Balmaceda and Coyhaique Alto are representative of this climatic zone. Finally, a fourth distinct zone might be considered the high elevation areas of the Andes. Generally, above 1500 meters there is no plant growth, little soil development and areas of permanent snow or glaciers (IREN-CORFO 1979). **Table 2**

presents some of the climatic differences between three key towns in the Aysén basin. It is noteworthy that snow and the number of days of sub-freezing temperatures becomes important over 500 m. There are no weather stations above 1000 m, representing the cold, alpine climate zone. **Fig. 5** shows the isohyets within the Aysén basin. The strong orographic (rain shadow) effect on precipitation is notable.

Table 2 – Climatic information for three towns within the Aysén Basin. They occur along the pronounced West – East gradient of climatic conditions occurring within the basin.

Parameter	Puerto Aysén	Coyhaique	Balmaceda
Elevation (meters)	10	275	520
Mean Annual Temperature °C	9	7.7	6.5
Months with minimum temperature <0°C	0	1.6	3.2
Days of snow per year	5.6	12	21
Annual Precipitation (mm)	2961	1349	611
Wind above 20 knots (days/year)	6	57	244
Overcast days (>6/8 of day with cloud cover)	278	213.6	59.7

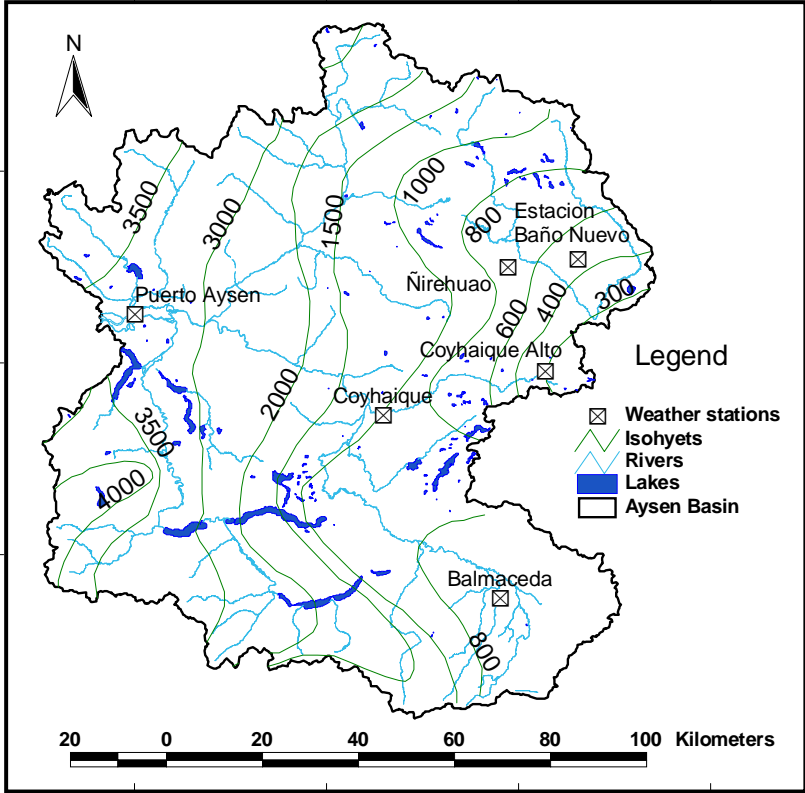


Fig. 5 – Weather stations and Isohyets (mm/yr) in the Aysén basin

2.6 Fluviometric regimes

Because all major subwatersheds within the Aysén basin contain a large range of elevations, they all receive precipitation as both snow and rain. However, one can make the distinction between the mixed regimes of the cold temperate zone where precipitation is plentiful and exhibits minimal seasonal oscillation and the area to the East of the main Andes range which exhibits a marked orographic effect. In this second zone, more precipitation falls during the winter, where it often falls as snow. Thus, we expect to see this reflected in the seasonal curve of streamflow for the different subbasins.

In **Fig. 6** the seasonal curve of the Aysén River measured in Puerto Aysén is shown. Flow rates of m^3s^{-1} were converted into $mm/year$ considering the area of the basin upriver of this station. The probability of the flow rate exceeding certain flows was graphed by month, as was the average precipitation of three rain gages in three climactic zones (blue line). This precipitation curve, while not representing the precise average for the entire basin, is meant to integrate values from different areas within the basin. **Fig. 7** shows the same analysis applied to the Simpson River just downstream from the confluence with Rio Coyhaique. This station measures the flow from a basin that generally lays to the East of the main Andes range and the effect of snowfall on the streamflow curve is notable during the months of snowmelt (September – December).

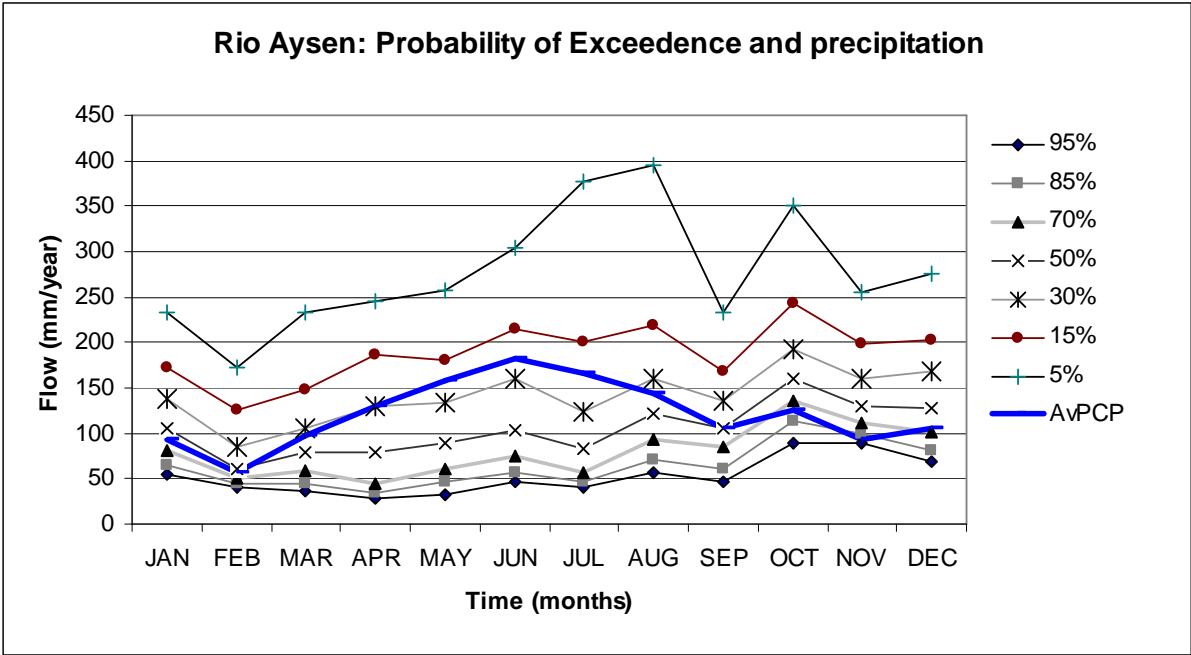


Fig. 6 – Fluviometry of the Rio Aysen: probability of exceedence

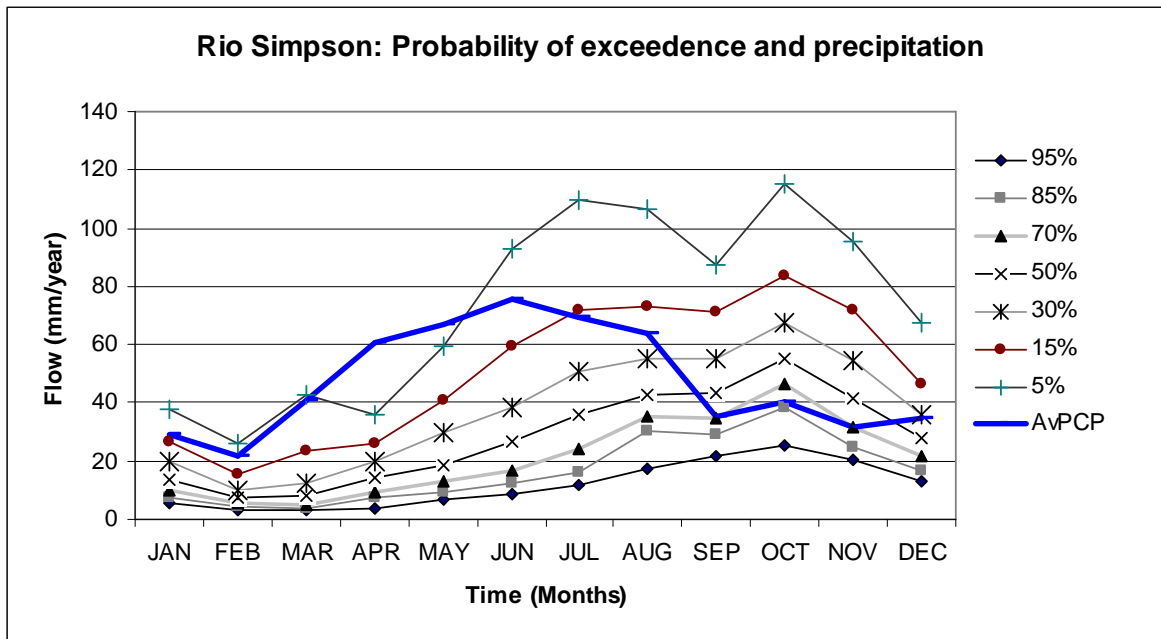


Fig. 7 – Fluviometry of the Rio Simpson: probability of exceedence

Finally, in light of the fact that this deliverable considers the solid phase of the hydrologic cycle, it is interesting to consider that the Aysén basin is located less than 100 km from the North Patagonia Icefield. Monitoring of the glaciers associated with this icefield indicates that between 1944/45 and 1995/96, the total area of ice lost due to recession and thinning was approximately 64 km², or 1.5% of the total area of the icefield (Aniya 1999). Because the long-term data point to a slight warming trend, we do not expect that there would be a net increase in permanent snow and ice within the watersheds studied.

3 Estimation of groundwater recharge

3.1 Introduction

The choice of a model or method to compute recharge derives from the conceptualization of the recharge process of a study area. This conceptualization is based on the physical system, its geometry, all the inputs and outputs of water and its locations. The computation of recharge is based on mass balances between water coming in, going out or being stored in the water system. These mass balances are generally water-mass balances but can also be any substance-mass balance diluted in water. Models to compute recharge may be grouped into mass balances above saturated zone and mass balances in the saturated zone. Only the water mass balances are considered.

The **water mass balances above the saturated zone** are predictive models as they quantify recharge by computing the processes prior to recharge occurrence (precipitation, infiltration, water stored in the surface and in the vadose zone). The **soil daily sequential water balance** is an

appropriate method to estimate deep percolation and hence recharge. This method requires knowledge of the climatic data to characterize precipitation and reference ET, and knowledge of medium characteristic parameters, that depend on the complexity of the selected model. These models allow for estimation of distributed recharge in a region, produce results by recharge episode and may be applied to any geological medium (intergranular, fissured, karstic or more than one type). However, the more general application is for intergranular, as the soil storage is more easily quantified, and preferential pathways are less important.

The **water mass balances in the saturated zone** are response models as they represent the reaction of the groundwater medium to the recharge process. Several methods are available depending on the hydrogeological setting, for instance: (1) surface flow hydrograph separation, (2) spring discharge quantification, (3) flow quantification in aquifer sections, (4) saturated zone storage change (water level change), (5) combination of these methods, also including human water abstractions. These methods are integrative for a region and may compute recharge by episode.

In the **surface flow hydrograph separation method** base flow and direct runoff are separated. Base flow is an estimate of recharge that occurs in the area defined by a watershed. Between the occurrence of the recharge process and the subsequent base flow, the process of discharge from the saturated groundwater medium to the surface medium must be considered.

Base flow is a measure of the groundwater medium discharge to the surface medium if: (1) there is no storage of surface water; (2) there is no evaporation of surface water; and (3) there is no abstraction of surface water. On the other hand, groundwater discharge may translate the groundwater recharge of a watershed if: (1) recharge is the only water source of the saturated medium; (2) there is no abstraction of groundwater; (3) all the water that leaves the saturated zone flows to the surface medium; and (4) there is no evapo(transpi)ration from groundwater.

The hydrogeological settings more favourable to observe this requisite are local systems of metamorphic and igneous rocks, with intergranular or fissured porosity. In some cases of sedimentary rocks with intergranular porosity, even if stratified, this requisite may still be found. The surface flow hydrograph separation method is probably the easiest recharge calculation method to use, as it does not require medium characteristic parameters, and only requires knowledge of daily precipitation and flow series.

The **spring discharge method** provides a direct measurement of the amount of water that recharged the system. It requires the knowledge of the area drained by the spring, which is not an easy value to obtain. Due to the structure of the groundwater flow paths and its significant water volumes this method is mainly applicable for karstic hydrogeological settings. For the other hydrogeological media,

despite the possible occurrence of large flow springs, it is likely that it exists diffuse discharge in important amounts which difficult the quantification of discharge.

The **flow quantification in aquifer sections** is applicable to any hydrogeological medium requiring the knowledge of the recharge area up-gradient of the measuring section, the constant monitoring of the piezometric level in both sides of the section and the aquifer transmissivity along the measuring section. These requirements turn the application of the method more difficult.

The **water level change** is a direct consequence of recharge. Time for the application of this method is very short. For the application of this method it is required that in a study volume, the difference between groundwater flow entering and leaving the system is negligible in relation to the water level rise. This method also requires the characterization of effective porosity in the depth of water level oscillation.

In this project the **surface flow hydrograph separation method** will be applied to two selected watersheds in the study area. Furthermore, because of the importance of snow in the Aysén Basin, a snowmelt model has been implemented for two watersheds and the results are used in the **surface flow hydrograph separation method**.

3.2 Surface flow hydrograph separation method

Surface or total flow (F) of a river is mainly composed of (1) direct runoff or overland flow (F_d), produced in the watershed above the place where it is measured, resulting from precipitation that does not infiltrate into the soil surface and that is not retained (for example in the plants canopy, buildings, dams, etc.), and (2) base flow (F_b), resulting from water that infiltrates into the soil, goes through the subsurface and eventually comes to the surface, being the discharge of groundwater to the watershed:

$$F = F_d + F_b \quad \text{Eq. 1}$$

The hydrograph represents surface flow against time (Fig. 8). The two large flow components of total flow (F_d and F_b) may be separated in the hydrograph. Several methods exist (*c.f. e.g. Linsley et al., 1975*). One of these, which is the basis of the methodology used in this study, consists in connecting total flow that exists in the beginning of the rising limb to the total flow that exists in the end of direct runoff. Linsley *et al.* (1975) present the following equation to estimate time from the hydrograph peak until a point located in the end of the recession curve that reflects the end of direct runoff (A is watershed area above the measuring station in km^2 and n is number of days):

$$n = 0,8 \cdot A^{0,2} \quad \text{Eq. 2}$$

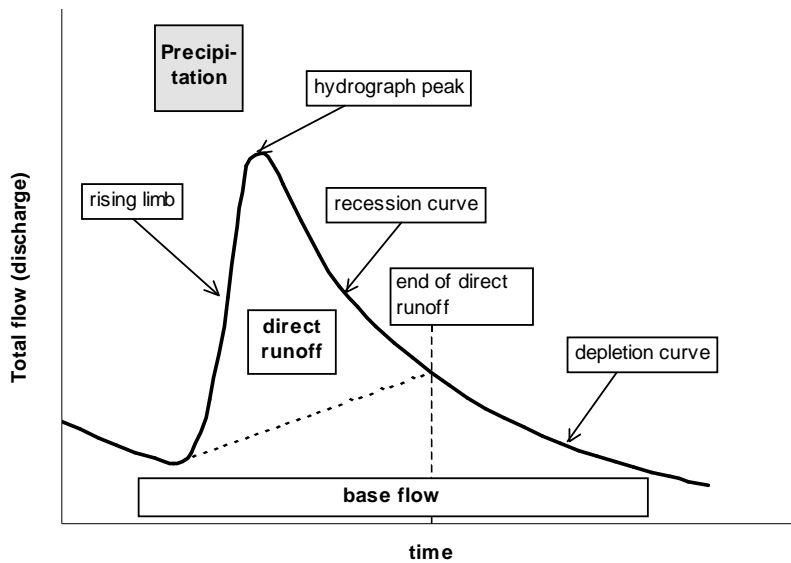


Fig. 8 – Method to separate total flow in direct runoff and base flow

The procedures developed for hydrograph separation (HS) use a daily time step and were programmed in DECHIDR_VB using Visual Basic 6.0 (Oliveira, 2001). The general technique for the separation follows the method represented in Fig. 9, though in this case the total flow in the beginning of the rising limb is always zero. The method consists in plotting a straight line linking the hydrograph origin of the precipitation/recharge (P/R) episode under analysis with total flow calculated in the beginning of day $n + 1$. Day n [computed with Eq. 2] refers to the number of days with direct runoff after the hydrograph peak [Fig. 9A] or the end of the precipitation if this exceeds the hydrograph peak [Fig. 9B]. The area above the line represents direct runoff of the episode under analysis while the area below the line represents its base flow.

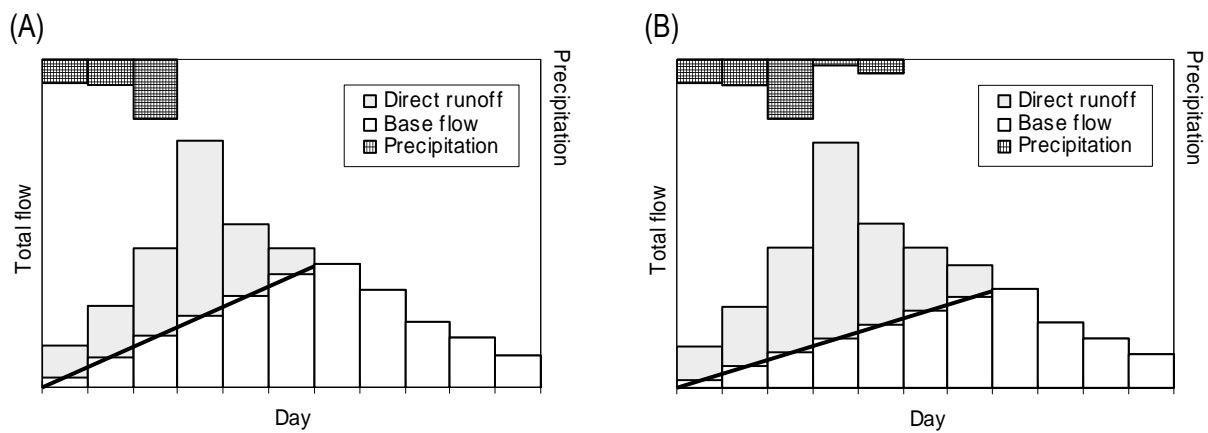


Fig. 9 – Example of the process of hydrograph separation, for $n = 2$ day, using as criterion (A) the day of the hydrograph peak, (B) the last precipitation day

Hydrograph separation turns to be a more complex process due to the occurrence of different superimposed episodes. The outcome is that in any given day the recession of several P/R episodes may be occurring. To deal with this situation, a set of procedures is developed in order to isolate distinct P/R episodes. The separation is carried out sequentially considering the input data series: date, total flow and precipitation.

The first step consists in determining the first day of a new P/R episode (episode B). Considering total flow existing since the beginning of the episode under analysis (episode A), it is considered that a new episode (episode B) starts when: (1) total flow is larger or equal to total flow in the previous day and total flow in the previous day is lower than total flow calculated two days before; (2) total flow is larger than total flow in the day before and this is equal to total flow calculated two days before. Depending on the selected option, the beginning of that episode is considered valid (1) in the day in which the previous conditions were met, independently of the occurrence of precipitation, (2) only in the first day of the rising limb after the day in which the previous conditions were met and the precipitation is larger than a precipitation threshold, defined as the minimum daily precipitation that must occur before direct runoff is generated.

Once the first day of the episode B has been established, the second step consists in determining the recession of episode A. To do this, a recession coefficient (α) of episode A is found by fitting a negative exponential curve of the type:

$$F = F_0 \cdot \text{EXP}(-\alpha \cdot t) \quad \text{Eq. 3}$$

to the flows of the recession or depletion periods in the days before the beginning of episode B. The parameter F is the total flow in the end of time t of the decreasing period and F_0 is the total flow when $t = 0$. The selection of the days used to compute α follows the criteria presented in Oliveira (2001). With the computed α , the water mass balance between the amount of precipitation that contributes to the episode and the corresponding total flow may be controlled. In this case, to accept α it is required that total flow is not larger than precipitation. If it is larger, a new α is searched that meets the equality between total flow and precipitation (see Oliveira, 2001).

The third step consists in calculating flow of episode A in the days that follow the starting of episode B, using **Eq. 3**, with F_0 given by total flow in the day before the starting of episode B.

The advantages of the HS method in estimating recharge are: (1) it is easy to apply with precipitation and flow data usually available; (2) only requires the definition of two parameters (1- number of days in which there is direct runoff, and 2- precipitation threshold – if this parameter is considered); (3) it is not constrained to fixed parameters of the watershed because each P/R episode is

considered separately; (4) it is able to control and maintain the mass balance between precipitation and the produced total flow; (5) it integrates all the processes of the hydrological cycle that take place in the watershed, measuring the response of the system to those processes; (6) it is applicable to the whole watershed, not requiring the definition of recharge and discharge areas of the groundwater medium.

The following limitations are referred to: (1) it is vulnerable to errors in the determination of total flow; (2) it is dependent on the as good as possible estimation of precipitation in the watershed, mainly if the balance between precipitation and total flow is used; (3) it considers that rivers are the only receiving bodies (does not consider bank storage) and that all groundwater discharges to those streams inside the watershed; (4) it may not be used directly if there are dams that inhibit natural flow.

3.3 Simple energy-budget snowmelt model

In many temperate regions of the world, snowmelt represents an important source of water and can, to varying degrees, change the patterns observed in hydrographs. Moreover, the chemical properties of meltwater change over the snowmelt period. Tracer studies are often used to illuminate the origin and principal flow paths of water in a basin (Sueker *et al.* 2000). Information on chemical tracers is not available for the Aysén basin, therefore simple energy-budget equations were used to predict the quantity and timing of snowmelt in specific watersheds.

Fig. 10 presents a simplified graphic of snowmelt and related processes. Snowmelt depends on the balance of a series of energy sources and sinks, including shortwave and longwave radiation, convection from the air (sensible energy), vapour condensation (latent energy), conduction from the ground, and the energy contained in rain (USACE 1998). Once snow melts, it can follow the same flow paths as rain. Thus, snowmelt calculations can effectively be separated from the processes related to the movement of the snowmelt into the river network.

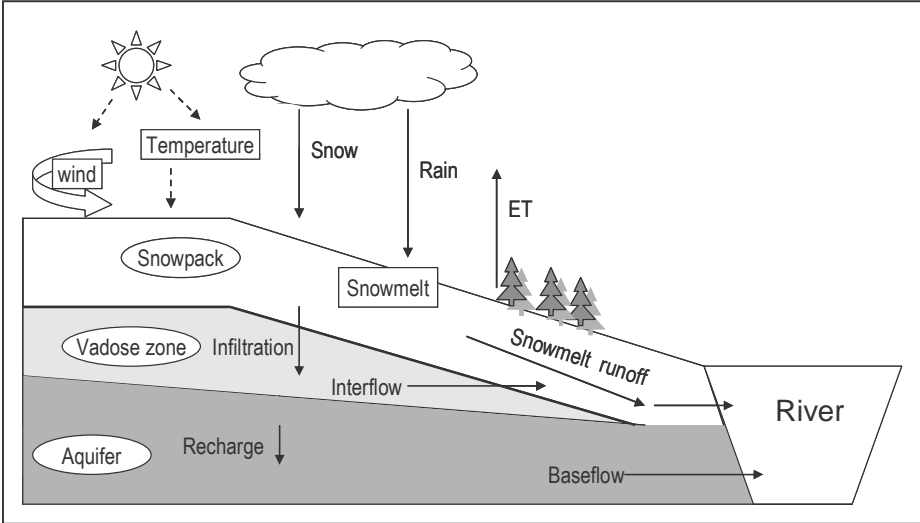


Fig. 10 – Schematic representation of main processes related to snowmelt.

The surface flow hydrograph separation method requires minimal data and is able to provide valuable information about the importance of base flow versus runoff in a watershed. The snowmelt model calculates precipitation as rain, new snow, snowpack, and ultimately meltwater. The water available for movement as base flow or surface flow (meltwater plus precipitation as rain) is calculated on a daily basis and imported into DECHIDR_VB in order to obtain values for base flow.

Two watersheds within the Aysén basin were chosen for application of the snowmelt model and the hydrograph separation method because they are gauged rivers and are close to weather stations. An additional consideration was a significant elevation range. Weather stations in the Aysén basin are generally located below 700 m elevation and in order to fully understand hydrographs in the basin it is necessary to consider the dynamics of snowfall and snowmelt at higher elevations. Each watershed was divided into three elevation bands of approximately 500 m each. This elevation range was suggested in the documentation for the Snowmelt Runoff Model (Martinec 1994). Furthermore, each watershed was divided into zones according to the dominant gradient in annual precipitation. For the Coyhaique watershed, the annual precipitation decreases from the fluviometric station, eastward toward Argentina. The Rio Claro watershed receives higher overall precipitation, decreasing from the headwater to the fluviometric station. Using routines in ArcView GIS 3.2, the area of each of these precipitation-elevation zones was calculated, as well as an estimation of the percent areal forest coverage. Forest cover data came from the spatially-explicit 'Catastro del Bosque Nativo' database generated by CONAF-CONAMA in 1997 and provided to ECOManage by SERPLAC. Information about the physiognomy of the vegetation in the watersheds was quantified using the **Table 3** and each vegetation type was weighted by its area within each zone. Canopy cover is important in the calculation of long-wave radiation, short-wave radiation, and convection melt. **Table 4** shows the categories of forest density used to determine which of the simplified energy-budget equations can be used.

Table 3 – Weighting factors for structural vegetation classes

Structural vegetation class	Weighting factor
Dense forest	1
Semidense forest	0.7
Open forest	0.4
Pine plantation	0.8
Semidense matorral	0.3
Open matorral	0.2
Rock outcroppings, pasture	0

Table 4 – Weighting factors for structural vegetation classes

Descriptive category	Mean canopy cover
Heavily forested	>80
Forested	60-80
Partly forested	10-60
Open	<10

(Source: USACE 1998)

The generalized energy-balance snowmelt equations are often simplified based on certain meteorological or forest-cover conditions. In general, we can divide snowmelt into two types: rain-free melt and rain-on-snow melt. Equations for the rain-on-snow melt can be greatly simplified because solar radiation can be considered a relatively minor energy input. The equations used to model snowmelt for the Rio Claro and Rio Coyhaique watersheds were taken from a 1998 US Army Corp of Engineers document about snowmelt modeling. **Table 5** lists parameters and variables required by the snowmelt equations and gives information about their sources and values.

$M = (3.38 + 0.0126P) * T_a + 1.3$	Eq. 4 (rain-on-snow, forested)
$M = (1.33 + 0.239kv + 0.0126P) * T_a + 2.3$	Eq. 5 (rain-on-snow, open and partially forested)
$M = k'(1 - F)(3.08I_i)(1 - a) + (1 - N)(0.96T_a - 21.34) + N(1.33T_c) + k(0.239v)(0.22T_a + 0.78T_d)$	Eq. 6 (rain-free melt, open)
$M = k'(1 - F)(2.43I_i)(1 - a) + k(0.239v)(0.22T_a + 0.78T_d) + F(1.33T_a)$	Eq. 7 (rain-free melt, partially forested)
$M = k(0.239v)(0.22T_a + 0.78T_d) + F(1.33T_a)$	Eq. 8 (rain-free melt, forested)
$M = 3.38(0.22T_a + 0.78T_d)$	Eq. 9 (rain-free melt, heavily forested)
Variables and Parameters	
a = average snow surface albedo	
F = average basin forest canopy cover, effective in shading the area from solar radiation, expressed as a decimal fraction	
I_i = Isolation (Solar radiation on a horizontal surface, MJ/m ²)	
k = basin convection-condensation melt factor	
k' = basin shortwave radiation melt factor	
M = snowmelt, mm/day	
N = estimated cloud cover expressed as a decimal fraction	
P = daily rainfall, mm/day	
T_a = difference between the air temperature measured at 3m and the snow surface temperature, °C	
T_c = difference between the cloud base temperature and the snow surface temperature, °C	
T_d = difference between the dew-point temperature and the snow-surface temperature, °C	
v = wind at 15m, km/hr	

Source (USACE 1998)

Fig. 11 – Equations used in snowmelt model

The equations in **Fig. 11** are advantageous in that they describe the important processes related to snowmelt rather than using an index such as air temperature. However, in the case of rain-free snowmelt with little canopy cover, the number of heat exchange processes is large and there are several variables and parameters that are often not readily available. In the watersheds modeled, the equations for forested and partially forested areas were used. In the case of zone F (>1200 m; ~1750 mm annual precipitation) in the Rio Claro watershed, the rain-free, open area equation should be used. However, the use of this equation requires two additional variables that are unavailable for this area; furthermore, because the zone only misses the canopy cover threshold by 2 percent, it is deemed that the equation for partially forested areas will suffice.

Table 5 – Source of parameters and variables used in snowmelt model

Parameter or variable	Source or References	Value (if applicable)	Considerations
Daily mean air temperature, °C	DGA		Average of daily min and max values
Dewpoint Temperature, °C	Relative humidity, temperature (DGA)		Relative humidity for the Coyhaique Alto station, taken from the Nirehuao station
Precipitation, mm	DGA		Snowfall often underestimated in rain gages: if precipitation falls as snow, it is multiplied by a factor of 1.3 (Larson and Peck 1974)
Temperature – Elevation Adjustment factor	SRM User Manual 1998	-0.65 °C/ 100m	Average temp for elevation zones is adjusted from nearest weather station
Precipitation adjustment factor	SERPLAC		Precipitation isohyets used to adjust the precipitation falling at nearest station. Number of rain days unchanged.
Wind (v)	DGA		Daily wind from Nirehuao used for the Coyhaique watershed, average monthly values used for the R. Claro watershed
Solar radiation	Monthly average hours of sun (DGA)		Solar radiation calculated on a monthly basis using Excel worksheet provided by IST.
Snow albedo (α)	Tague & Band 2004	$\alpha = 0.85(0.94^{Age^{0.58}})$	Albedo decay function based on the number of days since last snowfall
Mean elevations	DEM (SERPLAC)		Watershed divided into 3 elevation zones; mean elevation calculated in ArcView
Forest cover (F)	Land use GIS theme (SERPLAC)		Vegetation structural classes converted to forest cover categories with the weighting factors found in Table 3
Basin convection-condensation melt factor (k)	USACE 1998	0.5	Range is 0.3 to 1. A low value was used because of high forest and matorral cover in study watersheds.
Basin shortwave radiation melt factor (k')	USACE 1998	1	Range of parameter 0.9 to 1.1: a central value was used because aspects are evenly distributed in study watersheds

The snowmelt model was built in Microsoft Excel according to the flowchart in **Fig. 12**. It is important to note that snow was measured in units of water equivalent (mm) so as not to introduce further uncertainty as to snow depths and snowpack dynamics. Using information about temperature and precipitation for each zone, new snow was calculated daily. A daily snow balance equation was

used to calculate the evolution of the snowpack over time. The snowmelt calculated for either rain-on-snow or rain-free conditions was weighted by the area of snow coverage per elevation zone.

MODIS satellite images were classified in ENVI 4.2, using the middle infrared (mir) and blue bands (the bands used for the normalized difference snow index). A maximum likelihood supervised classification routine was used; the regions of interest for the supervised classification were based on a GIS coverage from SERPLAC indicating areas of permanent snow. Three MODIS images were used, representing winter (July 12 to 28, 2005), spring (November 12 – 28, 2005), and summer (March 6 – 21, 2006) (**Fig. 13**). A sinusoidal curve was fit to these few data points using the snow coverage for each elevation zone in the two watersheds. Using the equations thus produced, an attempt was made to use the daily proportion of each elevation zone covered by snow and a weighting factor for snow melt. This makes intuitive sense: as the area covered by snow in each zone decreases during the spring, the production of snowmelt water should decrease even as the rate of melt increases. However, the implementation of this snow-cover-area weighting factor was problematic. On one hand, **Fig. 14** and **Fig. 15** indicate that significant inter-annual variation can occur in these basins, thus the acquisition and analysis of MODIS images becomes labor-intensive. On the other hand, use of a weighting factor was shown to lead to significant snow accumulation between years in the Rio Claro watershed. In the absence of information indicating that there is net snow and ice accumulation in this watershed, it appeared judicious to not apply the snow-cover-area weighting factor until more information is available.

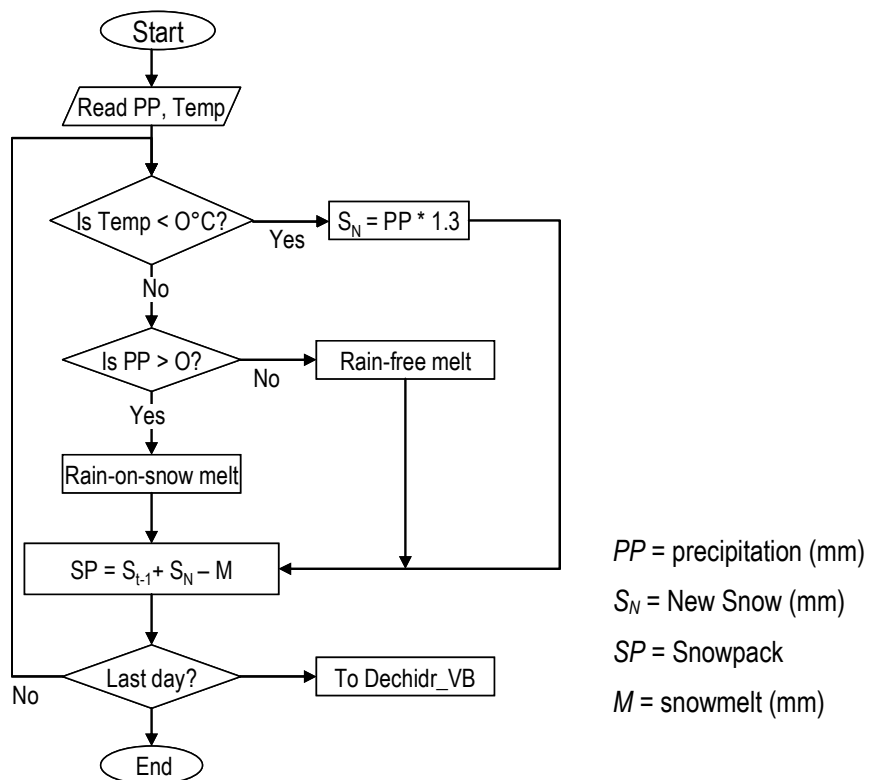


Fig. 12 – Flow chart for Snowmelt model

Finally, the daily snowmelt and the precipitation as rain were summed across each watershed to get the daily water available for infiltration (eventually baseflow) and direct runoff. This output was then formatted for use with the DECHIDR_VB model.

As recorded data were not available on snowfall, snow depth, and snow melting rates for the Aysén region, the snowmelt model could not be verified. A rudimentary calibration was undertaken by (1) comparing the snow-covered area generated from the MODIS images with the presence of snowpack in the elevation bands and (2) modifying the precipitation adjustment factors so that long-term precipitation was greater than the streamflow of the given watershed. The lack of a rigorous calibration of the snowmelt model should be taken into consideration when interpreting the final results.

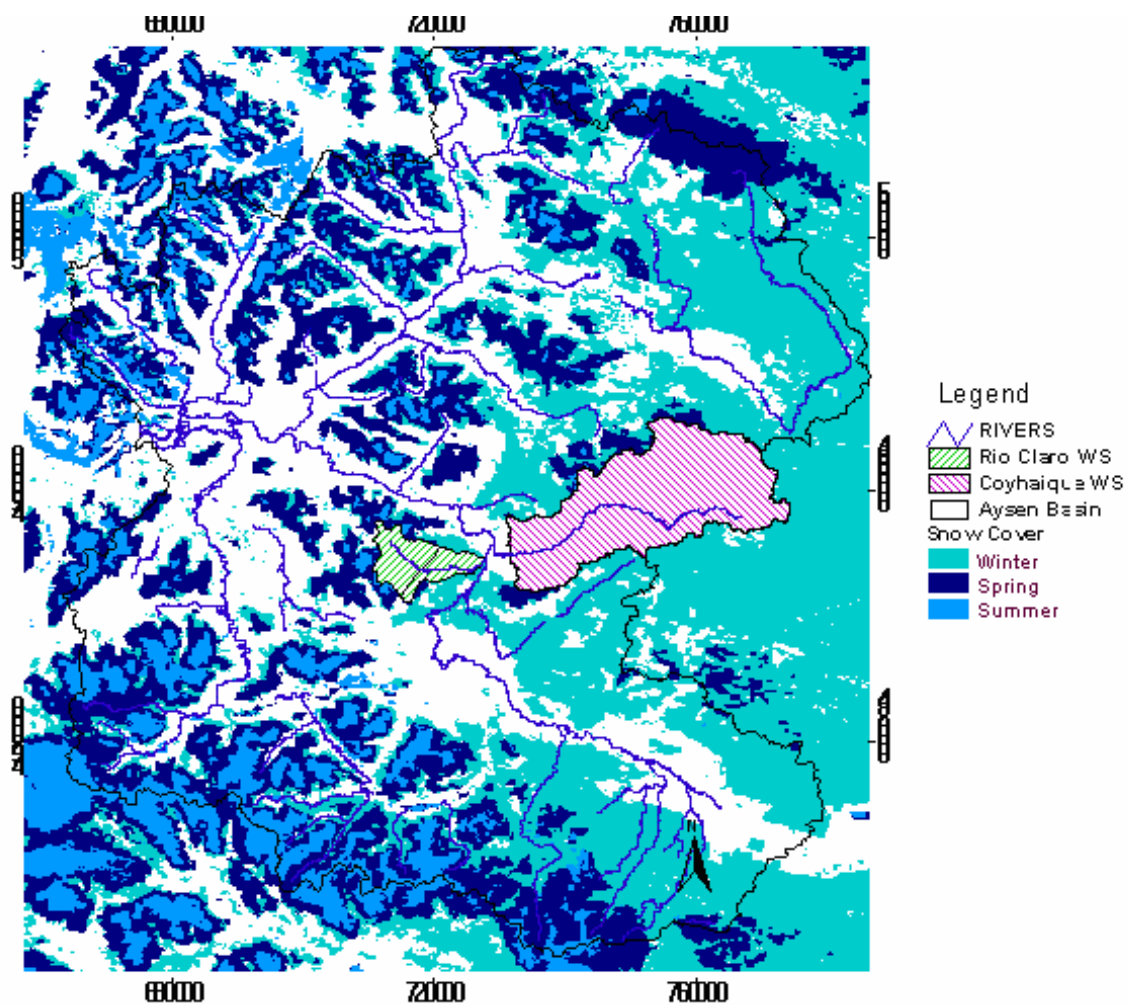


Fig. 13 – Snow cover winter – summer 2005- 2006. From MODIS imagery.

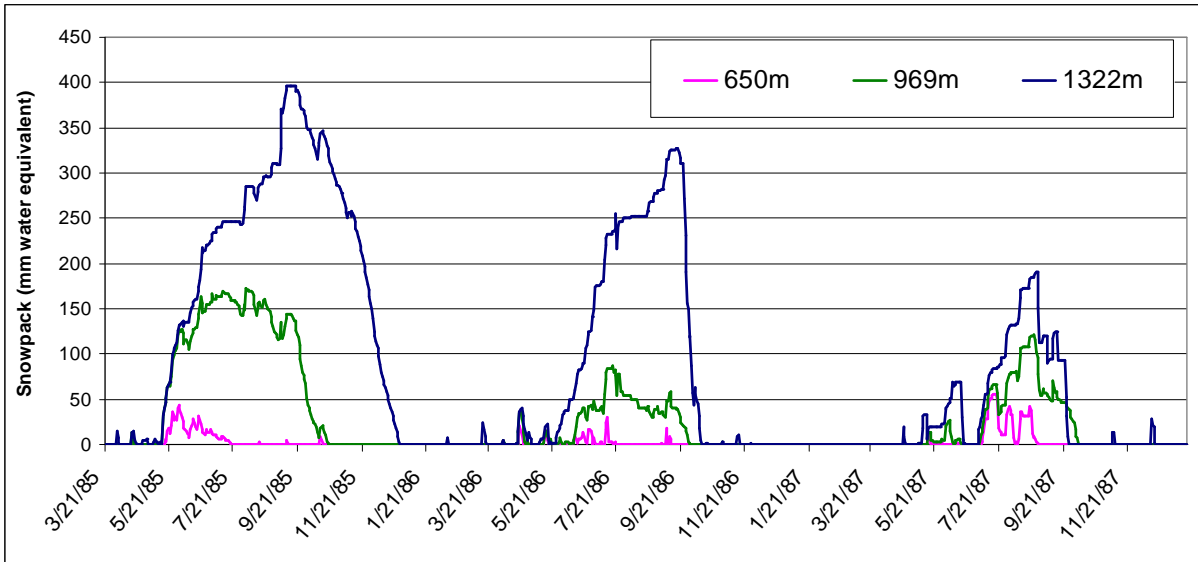


Fig. 14 – Modeled snowpack, Coyhaique watershed. Three vertical bands are shown; values are in mm of water equivalent.

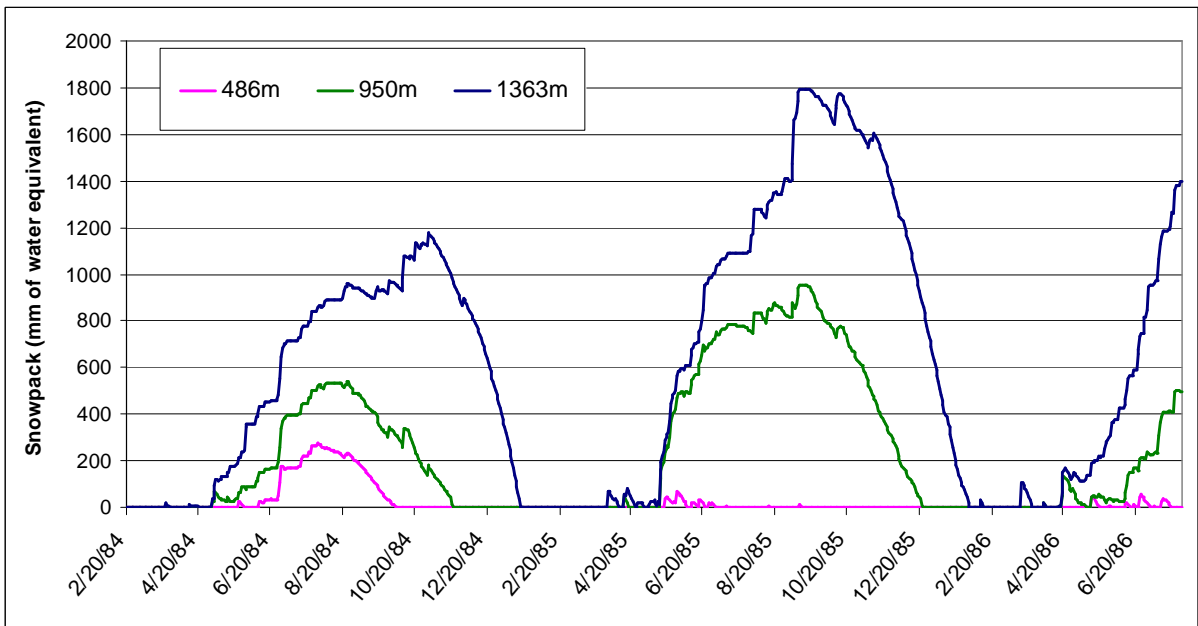


Fig. 15 – Modeled snowpack, Rio Claro watershed. Three vertical bands are shown; values are in mm of water equivalent.

A comparison of **Fig. 14** and **Fig. 15** shows that snow accumulation should be a more important process in the Rio Claro watershed, where up to 1800 mm of precipitation fell as snow in the highest elevation band. This significant accumulation of snow in the Rio Claro watershed also meant that snow remained on the ground longer into the summer than in the Coyhaique watershed, where the snowpack had melted between mid-October and early December.

3.4 Incorporating snowmelt in the hydrograph separation method

In basins where snow represents an important percentage of the annual precipitation, the unmodified use of the hydrograph separation method could lead to erroneous conclusions. Thus, it is important to consider how snowmelt might influence the hydrographs of the associated river and how to account for this process in the hydrograph separation method. **Fig. 16** indicates the two snowmelt scenarios considered in the snow model and their effect on the associated hydrograph. In **Fig. 16A**, a rain-on-snow event causes a large peak in the observed hydrograph. Although, DECHIDR_VB accepts one field for precipitation (or available water: snowmelt + precipitation as rain), the snowmelt model can give the proportion of snowmelt to rain on a daily basis and thus the results of DECHIDR_VB can be decomposed into components originating from snowmelt and from rain. Without accounting for snowmelt, baseflow would be overestimated. During the spring snowmelt season, one could expect hydrograph peaks solely due to snowmelt. If snowmelt is not separated from precipitation as rain, DECHIDR_VB would not necessarily consider such peaks as separate episodes, effectively underestimating runoff.

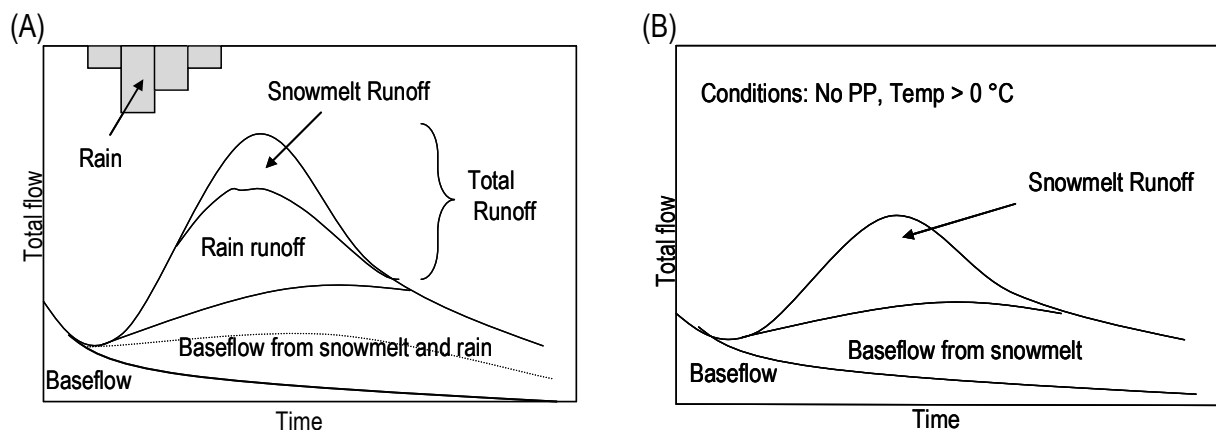


Fig. 16 – Hydrograph separation with snowmelt

3.5 Results of snowmelt and hydrograph separation models

3.5.1 Rio Claro Watershed

The Rio Claro watershed covers 108 Km² to the west of the town of Coyhaique. The Rio Claro flows toward the east, emptying into the Rio Simpson. With its headwaters coming from the central Andean range, this watershed has higher pluviosity and generally steeper slopes than the larger Coyhaique watershed. For the purpose of the snowmelt model, the watershed was divided into five zones, as seen in the **Table 6**. The available data allowed for the snowmelt model and DECHIDR_VB to be run for the following periods: May 1985 to December 1986 and December 2003 – August 2005.

Table 6 – Snowmelt model zones based on elevation and annual precipitation. The percent forest cover within each zone is indicated in parentheses.

Rio Claro Watershed			Coyhaique Watershed			
Elevation Zone (altitude m)	Precipitation (mm/yr)		Elevation Zone (altitude m)	Precipitation (mm/yr)		
	1200-1800	1800-2600		>800	400-800	<400
1 (226-699)	A (11.5%)	B (39.3%)	1 (282-799)	A (22.4%)	B (31.2%)	C (68%)
2 (700-1199)	C (74%)	D (68.9%)	2 (800-1249)	D (75.3%)	E (30.6%)	F (34.4%)
3 (1200-1722)		F (8.4%)	3 (1250-1697)	G (10.9%)	H (10.3%)	I (12.5%)

The hydrograph separation model, DECHIDR_VB, was run with the following settings: n (number of days from hydrograph peak until end of direct runoff) = 2; Minimum precipitation required to begin new recharge episode (mm); no control over balance between precipitation and runoff; model considers precipitation in order to start a new episode. In order to allow a comparison between dynamics with and without snowmelt, two runs were made for each period. A visual comparison of **Fig. 17** and **Fig. 18** indicates that with the calculation of snow melt, the interpretation of the hydrograph changes. In **Fig. 17** there is a steady contribution of snowmelt, with peaks of precipitation. It is likely that the daily snowmelt is not so constant. However, the snowmelt model uses monthly instead of daily radiation and thus differences between daily melt rates are probably less than what would be observed in the field. Nonetheless, the presence of this snowmelt water informs the hydrograph separation model that new runoff-recharge episodes should begin. Without this snowmelt signal (**Fig. 18**), the peaks in the hydrograph are considered to be due to baseflow – due to the fact that there is no precipitation as rain. Thus, the inclusion of snowmelt can (1) help explain the high streamflows and hydrograph peaks that occur in the absence of rain events and (2) help avoid the over estimation of baseflow when using the hydrograph separation method.

Monthly values for flows, precipitation and snowmelt for the two time periods modelled in the Rio Claro watershed are shown in **Table 7**. It is interesting that the average baseflow for this period represents close to 2/3 of the total streamflow. This is perhaps a surprisingly high value for a watershed that has relatively steep slopes and thus a large potential for high runoff rates. However, it must be considered that almost 40% of this watershed is covered by forest and that, in general, the soils are quite sandy (average of 88% sand in forest soils) (Cruces *et al.* 1999). Furthermore, the soils in the Aysén basin are often thin and underlain by weathered bedrock or glacial deposits (Hepp 1996), thus it makes intuitive sense that much of the streamflow in the Rio Claro watershed is contributed by shallow groundwater. However, it is important that the results be interpreted with caution as there is much uncertainty associated with the snowmelt model and the hydrograph separation method has several limitations (described in section 3.2).

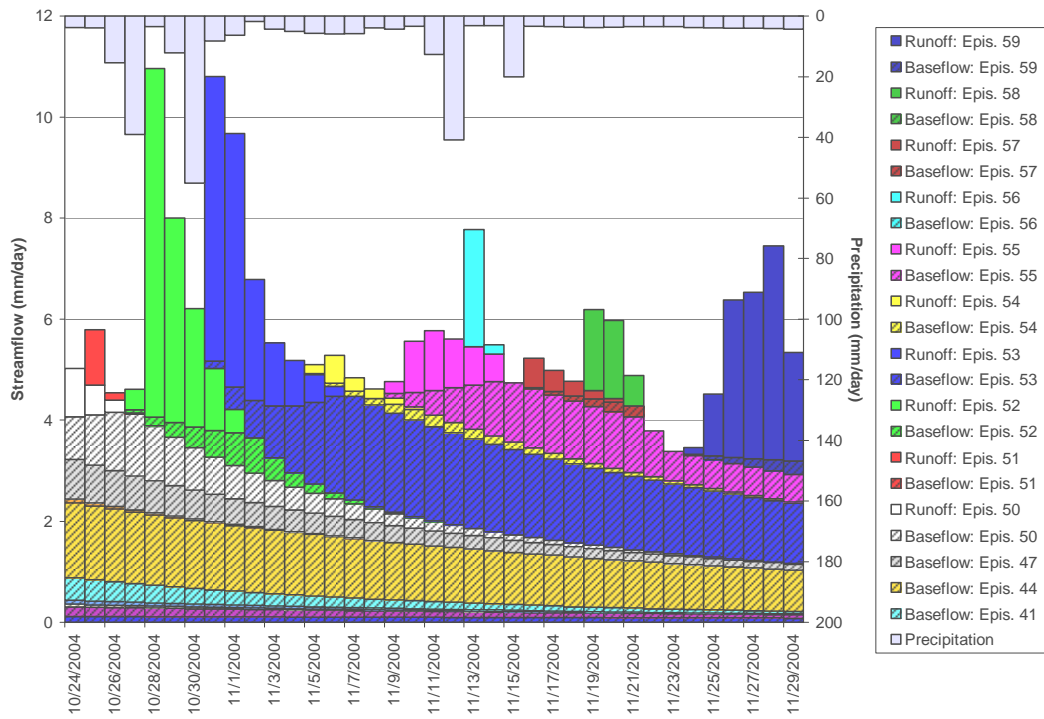


Fig. 17 – Hydrograph separation detail, Rio Claro watershed. The streamflow and precipitation (rain + snowmelt) are represented in units of mm/day. The shaded areas represent baseflow discharge, while the solid colors represent surface runoff.

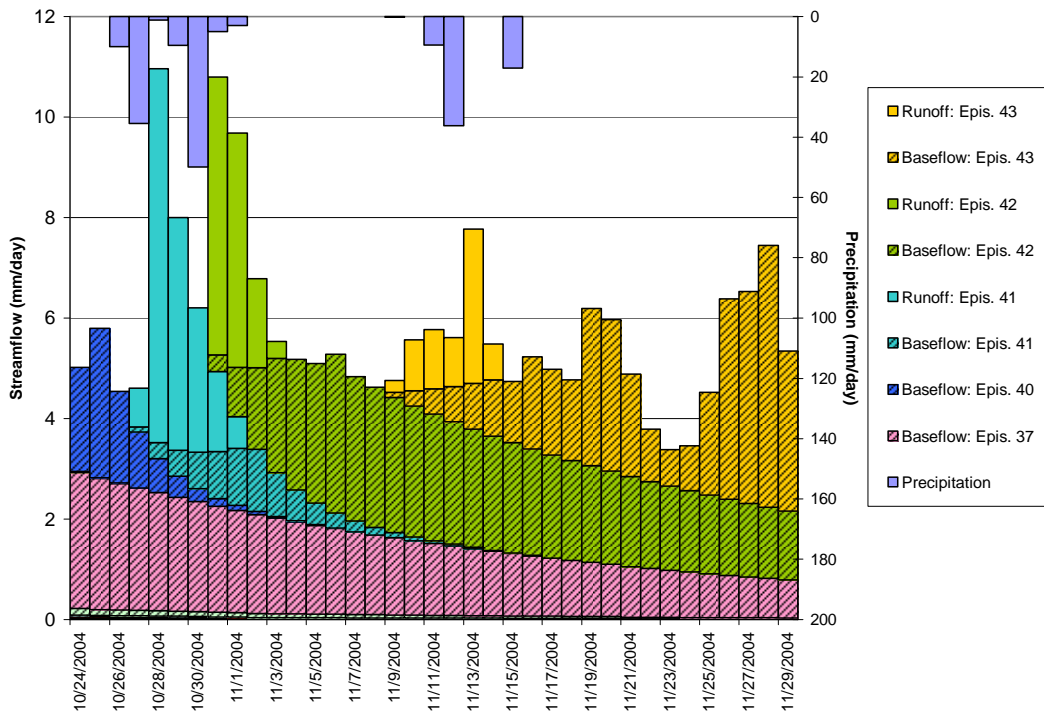


Fig. 18 – Hydrograph separation without snowmelt, Rio Claro watershed. The streamflow and precipitation (only rain) are represented in units of mm/day. The shaded areas represent baseflow discharge, while the solid colors represent surface runoff.

Table 7 – Monthly values for baseflow and associated variables, Rio Claro watershed.

All values are in mm/ month.

Date	Total Streamflow (F)	Baseflow (Fb)	Runoff (Fd)	Total Available Water (rain + snowmelt) (Tw)	Rain (R)	Snowmelt (Sm)	Fb/F (%)	Sm/Tw(%)
May-85	165	75	89	276	245	31	46%	11%
Jun-85	230	137	93	260	182	78	60%	30%
Jul-85	117	93	24	81	58	23	79%	28%
Aug-85	121	73	48	161	102	60	60%	37%
Sep-85	221	117	103	304	203	100	53%	33%
Oct-85	150	104	46	212	69	143	69%	68%
Nov-85	189	135	53	343	127	216	72%	63%
Dec-85	133	89	44	294	61	233	67%	79%
Jan-86	136	73	63	286	156	130	54%	45%
Feb-86	91	70	21	58	52	6	77%	11%
Mar-86	184	146	38	216	194	21	79%	10%
Apr-86	205	117	88	283	223	60	57%	21%
May-86	198	129	69	243	165	78	65%	32%
Jun-86	161	107	55	187	145	42	66%	22%
Jul-86	289	153	135	226	171	55	53%	24%
Aug-86	73	66	8	64	41	23	90%	35%
Sep-86	100	66	33	194	88	106	66%	55%
Oct-86	158	112	46	225	61	164	71%	73%
Nov-86	130	87	43	248	111	137	67%	55%
Dec-86	149	110	38	172	59	113	74%	66%
Dec-03	145	131	14	148	124	24	91%	16%
Jan-04	148	142	6	31	31	0	96%	0%
Feb-04	35	35	0	19	19	0	100%	0%
Mar-04	55	43	11	117	117	0	79%	0%
Apr-04	125	71	54	500	468	32	57%	6%
May-04	197	112	85	59	36	22	57%	38%
Jun-04	178	130	48	428	380	48	73%	11%
Jul-04	114	58	56	103	48	55	51%	54%
Aug-04	191	63	128	107	40	67	33%	63%
Sep-04	196	79	117	243	124	119	40%	49%
Oct-04	206	159	47	357	172	185	77%	52%
Nov-04	262	155	107	218	99	119	59%	54%
Dec-04	200	150	51	302	193	109	75%	36%
Jan-05	260	137	122	203	111	92	53%	46%
Feb-05	162	114	47	33	33	0	71%	0%
Mar-05	83	68	15	288	272	15	82%	5%
Apr-05	133	62	71	312	294	18	47%	6%
May-05	250	165	86	161	115	46	66%	29%
Jun-05	217	194	23	159	104	55	90%	35%
Jul-05	144	88	57	125	35	90	61%	72%
Aug-05	264	157	107	121	55	66	59%	54%
Average	165	107	58	204	131	73	65%	36%

Table 7 also indicates that snowmelt is an important component of runoff and baseflow. It appears that snowmelt regularly makes up between 50% and 70% of the water available for transport to

the river system during the spring months. This is important because it represents a significant time lag in watershed-level hydrodynamics that could ultimately play a role in the chemistry and sediment loads of the river water. Sueker *et al* (2000) indicate that during the snowmelt season in the Rocky Mountains, 42-57% of streamflow was provided by snowmelt runoff. If one considers that snowmelt can also infiltrate into the soil and ultimately contribute to baseflow, it is likely this percentage would be higher.

With the obtained values it was possible to construct the probability distribution function diagram that is shown in **Fig. 19**. The median base flow is 4.34 mm/d and the average base flow is 4.67 mm/d.

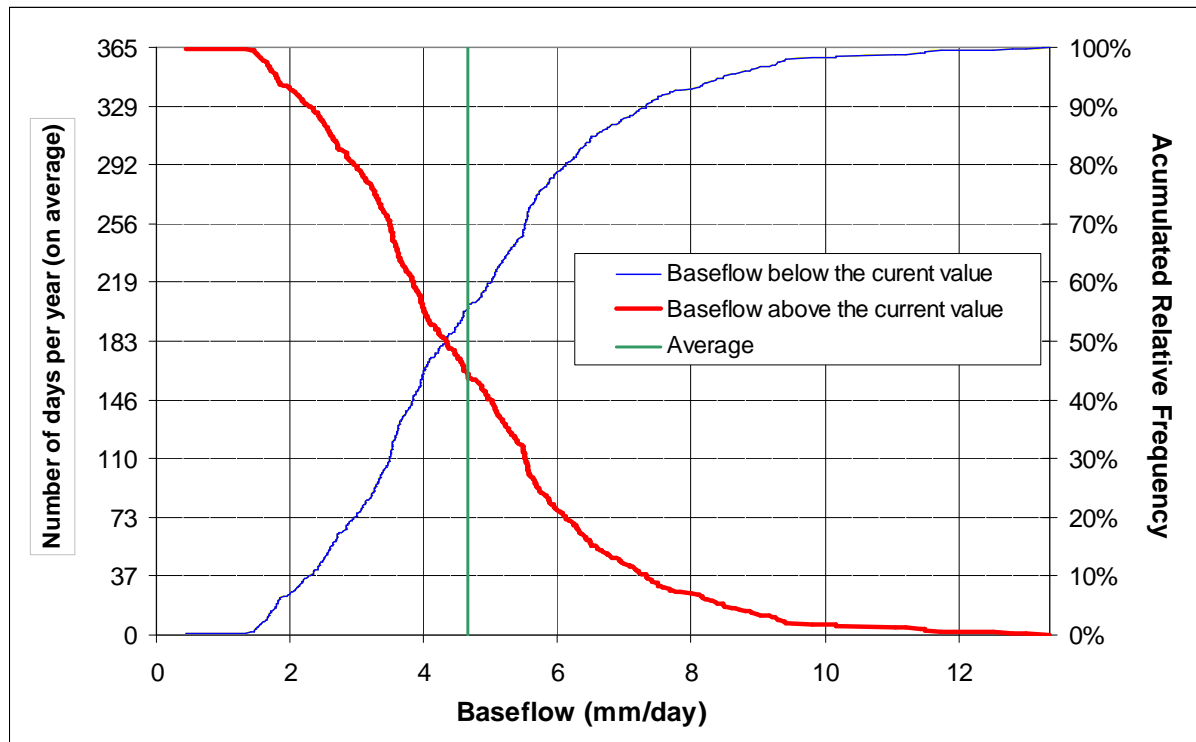


Fig. 19 – Probability distribution function of baseflow for Rio Claro watershed. **This figure is based on data from the period: December 2003 – August 2005.**

Assuming that the conditions referred to in section 3.1 are met, this base flow is an estimation of the recharge that occurred in the system.

3.5.2 Coyhaique Watershed

The Rio Coyhaique watershed covers 616 Km² to the east of the town of Coyhaique, where it flows into the Rio Simpson. The eastern margin of the Coyhaique watershed borders with Argentina and includes areas classified as Patagonian steppe. The eastern part of the watershed is quite dry (average annual precipitation of 325 mm) and it receives higher precipitation between May and August (winter). For the purpose of the snowmelt model, the watershed was divided into nine zones, as seen in the

Table 6. The available data allowed for the snowmelt model and DECHDR_VB to be run for the following periods: January 1985 to April 1986 and January 2000 – February 2003.

Table 8 – Monthly values for baseflow and associated variables, Coyhaique watershed
All values are in mm/ month.

Date	Total Streamflow (F)	Baseflow (Fb)	Runoff (Fd)	Total Available Water (rain + snowmelt) (Tw)	Rain (R)	Snowmelt (Sm)	Fb/F (%)	Sm/Tw(%)
Jan-85	13	11	2	22	22	0	83%	0%
Feb-85	7	6	1	20	20	0	87%	0%
Mar-85	8	7	1	21	21	0	91%	0%
Apr-85	23	15	9	68	58	10	62%	14%
May-85	39	30	10	64	45	19	75%	30%
Jun-85	108	75	33	93	41	52	69%	56%
Jul-85	81	74	6	36	13	24	92%	66%
Aug-85	81	68	13	59	28	32	84%	53%
Sep-85	136	95	41	107	53	55	70%	51%
Oct-85	149	110	39	51	16	35	74%	69%
Nov-85	110	88	22	48	29	19	80%	40%
Dec-85	28	28	1	32	21	11	97%	34%
Jan-86	12	11	1	35	35	0	89%	0%
Feb-86	8	8	0	13	13	1	95%	6%
Mar-86	23	14	9	47	44	3	60%	6%
Apr-86	48	32	16	84	49	35	67%	42%
Nov-00	42	29	12	33	32	1	70%	2%
Dec-00	28	22	6	74	74	0	79%	0%
Jan-01	23	17	6	85	85	0	75%	0%
Feb-01	24	18	7	47	47	0	72%	0%
Mar-01	63	42	21	85	85	0	66%	0%
Apr-01	20	19	1	16	15	1	97%	5%
May-01	27	19	8	59	42	16	71%	28%
Jun-01	46	39	7	46	24	22	84%	48%
Jul-01	51	46	5	15	5	10	90%	69%
Aug-01	57	40	17	95	36	59	70%	63%
Sep-01	73	54	19	68	23	44	74%	65%
Oct-01	78	62	15	34	7	27	80%	79%
Nov-01	22	22	0	21	20	1	98%	4%
Dec-01	11	10	1	22	22	0	92%	0%
Jan-02	7	6	1	38	38	0	83%	0%
Feb-02	4	4	0	54	54	0	95%	0%
Average	45	35	10	50	35	15	80%	26%

Table 8 shows that streamflow in the Coyhaique River is comprised of 80% baseflow discharge. This is higher than the Rio Claro watershed and indicates that there is relatively little runoff. Again, it is worth mentioning the high permeability of the soils in the Aysén basin. This fact, coupled with the flatter

topography and low precipitation of the Coyhaique watershed could explain this high baseflow value. The snowmelt appears to make up a relatively small portion of the streamflow, about 26%. Although little confidence can be placed in this value because of the unvalidated state of the snowmelt model, it appears reasonable. Snowmelt still influences the hydrograph of the Coyhaique river, but this influence is more temporally limited as compared to the Rio Claro watershed. In general, it is apparent that the Coyhaique watershed exhibits a strongly seasonal pattern where monthly streamflow and snowmelt rates are highly correlated ($r = 0.77$, $n = 32$). On the other hand, the monthly precipitation as rain calculated by the snowmelt model is not significantly correlated with streamflow ($r = -0.08$, $n = 32$). This is an interesting anomaly and likely has to do with high evapotranspiration during the summer and the fact that much precipitation falls as snow during the winter.

The probability distribution function diagram constructed for the Coyhaique watershed is shown in **Fig. 20**. The median baseflow is 0.76 mm/d and the average base flow is 0.93 mm/d. As mentioned above, considering that the conditions referred to in section 3.1 are met, these baseflow rates represent an estimation of the recharge that occurred in the system. Given that the near edges of the Coyhaique watershed and the Rio Claro watershed are only 4 km apart (and their geographic centers are roughly 40km apart) it is notable that the baseflow recharge rates differ so greatly.

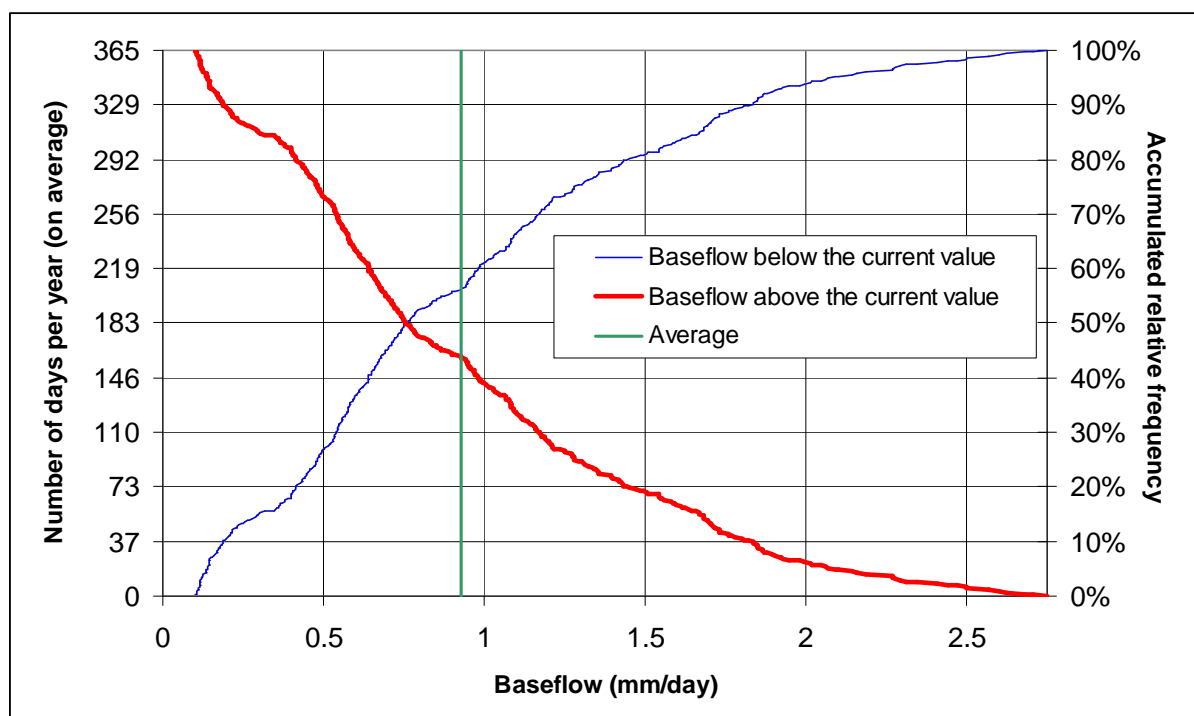


Fig. 20 – Probability distribution function of baseflow for Coyhaique watershed. **This figure is based on data from the period: January 2000 – February 2003.**

4 Groundwater vulnerability to pollution

4.1 Concept of vulnerability to pollution

The text presented in this and in the next section, was derived from Lobo Ferreira and Cabral (1991). It is believed that the most useful definition of vulnerability is one that refers to the intrinsic characteristics of the aquifer, which are relatively static and mostly beyond human control. It is proposed therefore that the groundwater vulnerability to pollution be defined, in agreement with the conclusions and recommendations of the international conference on "Vulnerability of Soil and Groundwater to Pollutants", held in 1987 in The Netherlands, as (Duijvenbooden *et al.*, 1987):

"the sensitivity of groundwater quality to an imposed contaminant load, which is determined by the intrinsic characteristics of the aquifer".

Thus defined, vulnerability is distinct from pollution risk. Pollution risk depends not only on vulnerability but also on the existence of significant pollutant loading entering the subsurface environment. It is possible to have high aquifer vulnerability but no risk of pollution, if there is no significant pollutant loading; and to have high pollution risk in spite of low vulnerability, if the pollutant loading is exceptional. It is important to make clear the distinction between vulnerability and risk. This because risk of pollution is determined not only by the intrinsic characteristics of the aquifer, which are relatively static and hardly changeable, but also on the existence of potentially polluting activities, which are dynamic factors which can in principle be changed and controlled.

Considerations on whether a groundwater pollution episode will result in serious threat to groundwater quality and thus to its (already developed, or designated) water supply are not included in the proposed definition of vulnerability. The seriousness of the impact on water use will depend not only on aquifer vulnerability to pollution but also on the magnitude of the pollution episode, and the value of the groundwater resource.

4.2 Methods for vulnerability assessment

Given the definition of vulnerability proposed as above, it is important to recognise that the vulnerability of an aquifer will be different for different pollutants. For example, groundwater quality may be highly vulnerable to the loading of nitrates at the surface, originated in agricultural practices, and yet be little vulnerable to the loading of pathogens.

In view of this reality, it is scientifically most sound to evaluate vulnerability to pollution in relation to a particular class of pollutant, such as nutrients, organics, heavy metals, pathogens, etc., *i.e.* to create specific vulnerability maps. This point of view has been expressed by other authors (*e.g.* Foster, 1987), and some work has been done in specific vulnerability mapping. An example is the work of Canter *et al.*, 1987 for nitrate pollution of agricultural origin. Alternatively, vulnerability mapping could be

performed in relation to groups of polluting activities (Foster, 1987), such as unsewered sanitation, agriculture, and particular groups of industries. This has been attempted for some activities. An example is the work of Le Grand (1983) for waste disposal.

Although it is recognised that this specific vulnerability mapping is scientifically sounder, one must realise that there will generally be insufficient available data to perform specific vulnerability mapping. Therefore, it is necessary to adopt a mapping system that is simple enough to apply using the data generally available, and yet is capable of making best use of those data in a technically valid and useful way. Various such systems of vulnerability evaluation and ranking have been developed and applied in the past. Examples are Albinet and Margat (1970), Haertl (1983), Aller *et al.* (1987), and Foster (1987).

Some of the systems for vulnerability evaluation and ranking include a vulnerability index which is computed from hydrogeological, morphological and other aquifer characteristics in some well-defined way. The adoption of an index has the advantage of, in principle, eliminating or minimising subjectivity in the ranking process. Given the multitude of authors and potential users of vulnerability maps in EU countries, Lobo-Ferreira and Cabral (1991) proposed for Portugal and the EU the definition of vulnerability in agreement with the conclusions and recommendations of the international conference on "Vulnerability of Soil and Groundwater to Pollutants", mentioned above, *i.e.* "*the sensitivity of groundwater quality to an imposed contaminant load, which is determined by the intrinsic characteristics of the aquifer*" and further suggested that a vulnerability index should be used for the vulnerability mapping to be developed for European Community Countries.

Such a standardised index has been adopted in the U.S., Canada and South Africa, and is currently used in those countries: the index DRASTIC, developed by Aller *et al.* (1987) for the U.S. EPA. This index has the characteristics of simplicity and usefulness.

4.3 The DRASTIC method

4.3.1 General description

The index of vulnerability DRASTIC (Aller *et al.*, 1987) was created for the following conditions:

- 1) the contaminant is introduced at the ground surface;
- 2) the contaminant is flushed into the ground water by precipitation;
- 3) the contaminant has the mobility of water; and
- 4) the area evaluated with DRASTIC is 100 acres (0.4 km²) or larger.

The index of vulnerability DRASTIC corresponds to the weighted average of 7 values corresponding to 7 hydrogeologic parameters:

- 1 - Depth to the water (D)

- 2 - Net Recharge (R)
- 3 - Aquifer material (A)
- 4 - Soil type (S)
- 5 - Topography (T)
- 6 - Impact of the unsaturated zone (I)
- 7 - Hydraulic Conductivity (C)

The DRASTIC index is a concept that joins several features that characterise the subsurface medium and its specificity (Fig. 21).

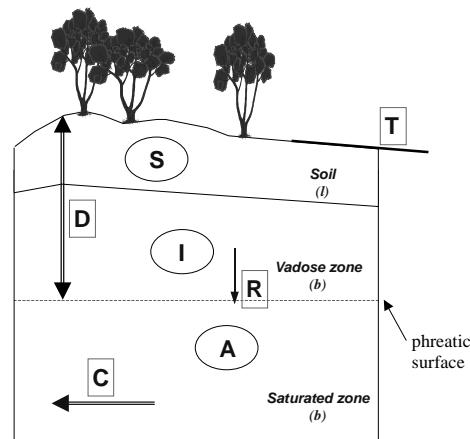


Fig. 21 - Parameters of the DRASTIC method

A value between 1 and 10 to each parameter, except R for which the value ranges between 1 and 9, is attributed, depending on local conditions. High values correspond to high vulnerability. The attributed values are generally obtained from tables, which give the correspondence between local hydrogeologic characteristics and the parameter value. Next, the local index of vulnerability is computed through multiplication of the value attributed to each parameter by its relative weight, and adding up all seven products:

$$DRASTIC = D_R D_W + R_R R_W + A_R A_W + S_R S_W + T_R T_W + I_R I_W + C_R C_W$$

where R = rating and W = weight.

Thus, each parameter has a predetermined, fixed, relative weight that reflects its relative importance to vulnerability. The most significant factors have weights of 5 and the least significant a weight of 1. A second weight has been assigned to reflect the agricultural usage of pesticides. In **Table 9** the factors are presented together with the weights respectively for standard DRASTIC applications and for DRASTIC pesticide applications.

The minimum value of the standard DRASTIC index is therefore 23 and the maximum value is 226. Such extreme values are very rare, the most common values being within the range 50 to 200.

Whereas the corresponding minimum and maximum values for pesticide DRASTIC index are 26 and 256 respectively.

Table 9 - Assigned weights for DRASTIC features used in Standard and Pesticide DRASTIC

Feature	Standard Weight	Pesticide Weight
Depth to Water (D)	5	5
Net Recharge (R)	4	4
Aquifer Media (A)	3	3
Soil Media (S)	2	5
Topography (T)	1	3
Impact of the Vadose Zone Media (I)	5	4
Hydraulic Conductivity of the Aquifer (C)	3	2

(Aller *et al.*, 1987)

Table 10 to **Table 16** show the ratings to be assigned to each parameter depending on the value that it assumes or the class to where it belongs. In some cases a rating interval and a typical rating is shown, which represents, in the case of the rating interval, the values that the parameter can assume, depending for instance on the clay content, the weathering conditions, or the fissuring in the case of the aquifer media.

4.3.2 Depth to the water (D)

The depth to water table is an important factor in the evaluation of groundwater pollution vulnerability primarily because it determines the thickness of material through which a contaminant must travel before reaching the aquifer. The depth to water table is also important because it provides an opportunity for oxidation and it may help to determine the contact time of pollutant with the surrounding media. In general, there is a greater chance for attenuation of pollutants to occur as the depth to the water table increases because deeper water levels imply longer travel times in the vadose zone with an exception that if the vadose media is fractured or karstified then the travel time is independent of the depth of water level. Because the DRASTIC was originally designed for evaluation of unconfined aquifers, special definitions must have to be assumed when evaluating depth to water for a confined aquifer. When an aquifer is confined, depth to water should be the depth to the top of the aquifer or base of the confining layer and therefore the measurements of depths to water levels in the piezometers do not provide the depth to water in confined aquifers. This parameter has to be derived from the geological cross sections and borehole data. In case of leaky confined aquifers the user has to treat such aquifers either as unconfined or fully confined based on the qualitative assessment of leakage quantity through the confining layer. Similarly in aquifers of large areas with varying degree of

confinement the user has to make appropriate decisions to assign spatially varying aquifer nature and hence spatially varying depths to water levels.

Table 10 shows the ratings to assign for the D parameter as a function of the depth to the water table in the case of an unconfined aquifer or the depth to the top of a confined aquifer.

Table 10 - Ranges and ratings for D - Depth to water

Range (feet)	Range (m)	Rating
0 - 5	0 - 1.5	10
5 - 15	1.5 - 4.6	9
15 - 30	4.6 - 9.1	7
30 - 50	9.1 - 15.2	5
50 - 75	15.2 - 22.9	3
75 - 100	22.9 - 30.5	2
> 100	> 30.5	1

(Aller *et al.*, 1987)

4.3.3 Net Recharge (R)

The quantity of net recharge represents the amount of water per unit area of land, which penetrates the ground surface and reaches the water table. The term net recharge is defined as the total quantity of water which is applied to the ground surface and infiltrates to reach the aquifer. This includes average annual infiltration amount and does not consider distribution, intensity or duration of recharge event like precipitation. This recharged water is thus available to disperse, dilute and transport a contaminant vertically into the vadose zone to the water table and horizontally within the aquifer. The greater the recharge, the greater the potential for groundwater pollution. However, at certain quantity of recharge the pollution event may in turn decrease due to dilution of the contaminant.

Table 11 shows the ratings to assign for the R parameter as a function of recharge values.

Table 11 - Ranges and ratings for R - net Recharge

Range (inches)	Range (mm)	Rating
0 - 2	0 - 51	1
2 - 4	51 - 102	3
4 - 7	102 - 178	6
7 - 10	178 - 254	8
> 10	> 254	9

(Aller *et al.*, 1987)

4.3.4 Aquifer media (A)

Aquifer media refers to a lithological unit that serves as an aquifer. Aquifer media plays an important role in dissipation and transportation of the pollutants once introduced into them. The parameters like effective porosity, grain size, clay contents and aquifer thickness are the four main characteristics that control dissemination and transportation of the contaminants in the saturated zone,

the aquifer. The effective porosity determines the travel time of the contaminant, higher the porosity faster the movement of the contaminant in the aquifer. The smaller grain size of the aquifer material provides for larger effective surface area for the contaminants to adsorb, exchange and disseminate in the aquifer. The clay is well known for its ion exchange capacity and if an aquifer has some clay content in it, then the contaminants would generally react with it and exchange some of the ions thereby reducing the contaminant concentrations. Therefore when looking into the aquifer media for assigning a DRASTIC rating one should look into the overall aspects of aquifer material in terms of its texture, composition, physical properties (especially effective porosity) and also clay content.

Table 12 shows the ratings to assign to parameter A depending on the aquifer material. A rating and a typical rating are shown. The rating is represented by an interval, which represents the values that the parameter can assume, depending for instance on the clay content, the weathering conditions, or fissuring. The typical rating is an average value and should be used if no more detailed information about the aquifer material is available.

Table 12 - Ranges and ratings for A - Aquifer media

Range	Rating	Typical Rating
Massive Shale	1 - 3	2
Metamorphic/Igneous	2 - 5	3
Weathered Metamorphic/Igneous	3 - 5	4
Glacial Till	4 - 6	5
Bedded Sandstone, Limestone and Shale Sequence	5 - 9	6
Massive Sandstone	4 - 9	6
Massive Limestone	4 - 9	6
Sand and Gravel	4 - 9	8
Basalt	2 - 10	9
Karst Limestone	9 - 10	10

(Aller *et al.*, 1987)

4.3.5 Soil media (S)

Soil media refers to that uppermost portion of the vadose zone which is characterised by significant biological activity. In the DRASTIC classification, the soil media is referred to be the upper weathered zone of the earth which averages to a depth of two metres or less from ground surface. Eleven different soil types which were given ratings of between 1 and 10 were defined by Aller *et al* (1987) – **Table 13**.

Table 13 - Ranges and ratings for S - Soil media

Range	Rating
Thin or Absent	10
Gravel	10
Sand	9
Peat	8
Shrinking and/or Aggregated Clay (montmorillonite or smectite clays)	7
Sandy Loam	6
Loam	5
Silty Loam	4
Clay Loam	3
Muck	2
Nonshrinking and Nonaggregated Clay (Kaolinitic or illitic clays)	1

(Aller et al., 1987)

4.3.6 Topography (T)

The term topography refers to the slope and slope variability of the land surface. Topography has an influence on the soil development and therefore has an effect on contaminant attenuation. The topography also determines the contact time of contaminants with the soil and in case of unconfined aquifers the topography can provide information about the groundwater gradients and velocities. Smaller ground slopes are always potential for groundwater pollution compared to steep slopes. It has been found that the grounds with 0 to 2 percent slopes provide the greatest opportunity for the contaminants to infiltrate because of low surface runoff and large contact time between the contaminant and the ground.

In DRASTIC method percent slope is considered for rating topography, which is equal to the vertical "rise" divided by the horizontal "run" (gradient of ground level). The classes and ratings to apply are given in **Table 14**.

Table 14 - Ranges and ratings for T – Topography

Range (Percent Slope)	Rating
0 – 2	10
2 – 6	9
6 – 12	5
12 – 18	3
> 18	1

(Aller et al., 1987)

4.3.7 Impact of the vadose zone media (I)

By definition, the vadose zone includes all the unsaturated media below the ground and above the water table, including the soil zone. As the soil was already considered in the S parameter, the I parameter of the DRASTIC method will refer only to the unsaturated media below the bottom of the soil

layer and above the water table in case of unconfined aquifer. Where an aquifer is confined, the extent of vadose zone includes all media below the bottom of the soil layer and above the top of the confined aquifer. In many situations, the vadose zone will not be a true vadose zone, because part of the saturated media may have to be treated as the vadose zone. When evaluating a confined aquifer, the “confining layer” must be treated as a vadose zone and be always assigned a rating of 1. The type of vadose zone media determines the attenuation characteristics of the material below the soil horizon and above the water table. Biodegradation, neutralisation, mechanical filtration, chemical reactions, volatilisation and dispersion are the processes that may occur within the vadose zone. The amount of biodegradation and volatilisation however, decreases with depth. The media also controls the path length and routing, thus affecting the time available for attenuation and the quantity of material found. The routing is strongly influenced by any fracturing present in the vadose media.

As for the A parameter, for each material it was considered a rating interval and a typical rating. The ratings and typical ratings are presented in **Table 15**.

Table 15 - Ranges and ratings for I - Impact of the vadose zone media

Range	Rating	Typical Rating
Confining Layer	1	1
Silt/Clay	2 - 6	3
Shale	2 - 5	3
Limestone	2 - 7	6
Sandstone	4 - 8	6
Bedded Limestone, Sandstone, Shale	4 - 8	6
Sand and Gravel with significant Silt and Clay	4 - 8	6
Metamorphic/Igneous	2 - 8	4
Sand and Gravel	6 - 9	8
Basalt	2 - 10	9
Karst Limestone	8 - 10	10

(Aller *et al.*, 1987)

4.3.8 Hydraulic Conductivity of the aquifer (C)

The rate of contaminant movement in the saturated zone is also controlled by the rate of groundwater movement. The parameter aquifer hydraulic conductivity is used to measure the rate of water flow in the aquifer. By definition the aquifer hydraulic conductivity is the ability of the aquifer to transmit water. The higher the conductivity the higher the rate of contaminant movement. The hydraulic conductivity is the result of the interconnected pores (effective porosity) in the sediments and fractures in the consolidated rocks.

Table 16 shows the ratings to assign for the C parameter as a function of the hydraulic conductivity.

Table 16 - Ranges and ratings for C - Hydraulic conductivity

Range (gpd/ft ²)	Range (m/d)	Rating
1 - 100	0 - 4.1	1
100 - 300	4.1 - 12.2	2
300 - 700	12.2 - 28.5	4
700 - 1000	28.5 - 40.7	6
1000 - 2000	40.7 - 81.5	8
> 2000	> 81.5	10

(Aller *et al.*, 1987)

4.4 Potential for the application of the DRASTIC method in Aysén

4.4.1 Depth to the water (D)

There exists no comprehensive data base on groundwater depth within the Aysén basin. The only potential source of information for parameter D is a series of petitions for groundwater pumping permits submitted to the DGA (Dirección General de Aguas) of the XI region. Unfortunately this information has not been converted to a digital format and it does not appear that the DGA considers this a priority. Until an ECOManage representative is able to travel to the region, this information is effectively inaccessible.

4.4.2 Net Recharge (R)

The only information on net recharge that has come to the attention of the author is the estimates reported in section three of this deliverable. This information is not spatially explicit, however, and is thus not ideal for mapping purposes.

4.4.3 Aquifer media (A)

Because parameters like effective porosity, grain size, clay contents are related to the lithological unit that serves as an aquifer, the ratings for the saturated zone (A) can be estimated from a geological map. For the Aysen basin, there are essentially two geological maps. One is a 1:1,000,000 scale map of the main geological units of the entire country. The second is a 1:100,000 scale map of the area between Coyhaique and Balmaceda which covers the southeast part of the Aysen basin. This map has a resolution that makes it useful for the application of DRASTIC, however it includes few complete subwatersheds within the basin.

4.4.4 Soil media (S)

The most comprehensive data set on soils is the IREN-CORFO study of 1979. However, it is quite descriptive in nature and does not provide quantitative data on soil texture and other important parameters. Furthermore, this study examined the soils of potentially arable lands and pasture lands,

leaving a notable void in the description of forest soils. Other soil information does exist, the SAG (Servicio Agrícola y Ganadero) office of the XI region apparently has collected a good amount of soil data. ECOManage-Chile is currently in the process of signing an agreement with the SAG in order to obtain this information. Through personal communication with SAG personnel, it appears that an unknown number of sample sites are not properly georeferenced, making the associated data useless for the purposes of DRASTIC application.

4.4.5 Topography (T)

This parameter is perhaps the best supported by available information. ECOManage has a DEM that has been calibrated for the Aysén basin and can be readily used to calculate slope classes.

4.4.6 Impact of the vadose zone media (I)

This parameter characterizes the unsaturated zone below the soil. The Coyhaique-Balmaceda Geological map can be used to estimate the ratings for this parameter. Additionally there is a GIS layer obtained from SERPLAC that characterizes the geomorphology of the Aysén basin. When used in conjunction with the geological map, this parameter should be calculable. One consideration is that in the areas of high precipitation, there may not exist a true vadose zone as conceptualized by the DRASTIC index. In these cases, it is likely that the bottom of the soil profile is permanently saturated.

4.4.7 Hydraulic Conductivity of the aquifer (C)

Again it is worth mentioning the applications for groundwater pumping filed with the DGA in the Aysén region. There exists a possibility that some of the information contained in these applications could allow the estimation of the hydraulic conductivity of the aquifer. However, accessing this information remains difficult.

Probably the only option currently available to estimate this parameter would be the use of the geological map mentioned above.

5 Conclusions

The Aysén basin of southern Chile presents a challenging case for the study of hydrogeology. Due to the fact that the population of the region is sparse and the precipitation is generally plentiful, there has been no need – either for agricultural, industrial or potable water purposes – for systematic investigation into the groundwater resources of the region. Thus there exists a veritable void in terms of empirical data on groundwater dynamics in the Aysén basin. This deliverable represents an attempt to establish the importance of groundwater in basin. The surface flow hydrograph separation method proved to be useful, as it requires only precipitation and streamflow data. However, the observation of distinct snowmelt regimes within the basin impedes the direct application of this method. The contribution of this deliverable is the linking of the hydrograph separation method with a daily snowmelt model that accounts for the time lag and distinct pattern in which precipitation becomes available for runoff or groundwater recharge. This model was based on available information about the topography, vegetation cover, and several meteorological and climatic variables. Unfortunately information that would allow a thorough calibration and validation of this model are not available.

Groundwater recharge estimates varied greatly between the Rio Claro watershed (average baseflow is 4.67 mm/d) and the Coyhaique watershed (average baseflow is 0.93 mm/d). This reflects the steep gradient in precipitation caused by an orographic effect as prevailing winds pass across the Andes. In all likelihood, this difference also reflects differences in topography and vegetation cover. In general, the baseflow was the major contributing component to streamflow. This underlines a need to undertake further study of ground water dynamics in the Aysén basin, especially in areas where there is a risk of groundwater pollution from point of diffuse sources.

A brief analysis of the potential for application of the DRASTIC index in the Aysén watershed was carried out. Only parameter T can be said to be solidly supported by available data; parameters R, A, S, I, C can be estimated from the geological map or other sources; no information exists for parameter D. D could be estimated by talking to professionals from the region that have some knowledge of the soils or hydrology. In conclusion, DRASTIC could probably be applied in a tentative fashion and may serve to highlight areas to conduct further hydrogeological work in the future.

VISAS



J.P. Lobo Ferreira
Groundwater Division Head
Laboratório Nacional de Engenharia Civil

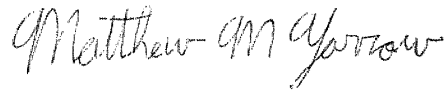


Rafaela de Saldanha Matos
Hydraulics and Environment Department Head
Laboratório Nacional de Engenharia Civil



Víctor H. Marín
Laboratorio de Modelación Ecológica Head
Departamento de Ciencias Ecológicas
Facultad de Ciencias, Universidad de Chile

AUTHORS



Matthew Yarrow
Dr. (c) en Ecología
Laboratorio de Modelación Ecológica
Facultad de Ciencias, Universidad de Chile



Manuel Mendes Oliveira
Ph.D. in Hydrogeology, Research Officer
Laboratório Nacional de Engenharia Civil

6 Bibliography

Albinet, M. and Margat, J. (1970) – "Cartographie de la vulnérabilité a la pollution des nappes d'eau souterraine", Bull. BRGM 2me Series 3 (4).

Aller, L.; Bennet, T.; Lehr, J.H.; Petty, R.J. and Hackett, G. (1987) – "DRASTIC: a standardized system for evaluating groundwater pollution potential using hydrogeologic settings". U.S. EPA Report 600/2-85/018.

Aniya M (1999) Recent glacier variations of the Hielos Patagónicos, South America, and the contribution to sea-level change. *Artic, Antarctic, and Alpine Research* 31:165-173.

CADE-IDEPE 2004. 'Diagnostico y Clasificación de los Cursos y Cuerpos de Agua Según Objetivos de Calidad: Cuenca del Río Aysén'. Consultancy report for the DGA.

CEA Ltda (2005) Revisión Base Datos Hábitat Acuático Dulceacuícola. Proyecto ECOManage

DGA (2005). Fluviometric Data for the Aysén Basin. Information provided as part of an accord between DGA and ECOManage –Chile.

Canter, L.; Knox, R. and Fairchild, D. (1987) – "Ground water quality protection". Lewis Publishers, Inc., Chelsea, Mi., 1987.

Cruces P., P, M Ahumada C. J Cerda C., F Silva L. (1999) Guía descriptiva de sitios misceláneos para la conservación y menor valor forrajero de la región de Aysén. Gobierno Regional de Aysén. Ministerio de Agricultura Servicio Agrícola y Ganadero (SAG). Departamento de Protección de los Recursos Naturales Renovables. Proyecto FNDR - SAG XI Región de Aysén: "Levantamiento Para el Ordenamiento de los Ecosistemas De Aysén"

Duijvenbooden, W. VAN and Waegeningh, H.G. van (1987) – "Vulnerability of soil and groundwater to pollutants". Proceedings and Information No. 38 of the International Conference held in the Netherlands, in 1987, TNO Committee on Hydrological Research, Delft, The Netherlands.

Foster, S.S.D. (1987) – "Fundamental concepts in aquifer vulnerability, pollution risk and protection strategy", in W. van Duijvanbooden and H.G. van Waegeningh (eds.), *Vulnerability of Soil and Groundwater to Pollution*, Proceedings and Information No. 38 of the International Conference held in the Netherlands, in 1987, TNO Committee on Hydrological Research, Delft, The Netherlands.

Gutierrez F, A Gioncada, O Gonzalez Ferran, A Lahsen, R Mazzuoli (2005) The Hudson Volcano and surrounding monogenetic centres (Chilean Patagonia): An example of volcanism associated with ridge–trench collision environment. *Journal of Volcanology and Geothermal Research* 145: 207– 233

Haertle, A. (1983) – "Method of working and employment of EDP during the preparation of groundwater vulnerability maps". IAHS Publ. 142(2).

Hepp, C. (1996) Praderas en la zona austral: XI Región (Aysén). In: INIA, Praderas para Chile. Editorial Ruiz.

IREN-CORFO (1979) Suelos y erosión. M. Peralta, S. Gonzalez, A. Carpinelli y A. Kühne (eds.). Perspectivas de desarrollo de los recursos de la Región Aysén del General Carlos Ibañez del Campo. Publicación N° 26, Tomos I y II. Santiago, Chile.

Larson, L.L., and E.L. Peck (1974) Accuracy of precipitation measurements for hydrologic modeling. *Water Resources Research* 10:857-863.

Le Grand, H.E. (1983) – "A standardized system for evaluating waste disposal sites". NWWA, Worthington, Ohio, 1983.

Linsley Jr, R.K.; Kohler, M.A. and Paulhus, J.L.H. (1975) – "Hydrology for Engineers". 2nd edn. McGraw Hill Kogakusha, Ltd.

Lobo Ferreira, J.P.C. and Cabral, M. (1991) – "Proposal for an operational definition of vulnerability for the European Community's Atlas of Groundwater Resources", in Meeting of the European Institute for Water, Groundwater Work Group Brussels, Feb. 1991.

Martinec, J., A. Rango and R. Roberts. 1994. The Snowmelt-Runoff Model (SRM) Users Manual, Updated Edition 1994, Version 3.2, Department of Geography - University of Bern.

Montgomery DR, G Blaco, SD Willett (2001) Climate, tectonics, and the morphology of the Andes *Geology*. 29: 579–582.

Oliveira, M.M. (2001) – "A Estimativa da Recarga das Águas Subterrâneas a Partir da Decomposição de Hidrogramas de Escoamento Superficial – O Programa de Computador DECHIDR_VB.VBP". Seminário sobre "A Hidroinformática em Portugal", Publicação em CD-ROM, LNEC, Lisboa, 15-16 Novembro, 2001.

Rosenau, MR (2004) Tectonics of the Southern Andean Intra-arc Zone (38° - 42°S). Dissertation: Freie Universität Berlin. <http://www.diss.fu-berlin.de/2004/280/index.html>.

SILVA, F., AHUMADA y M. CERDA, J. (1999) Guías de condición para los pastizales de la Ecorregión Templada Intermedia de Aysén. Proyecto SAG-Gobierno Regional de Aysén "Levantamiento para el Ordenamiento de los Ecosistemas de Aysén".

Sueker JK, JN Ryan, C Kendall, RD Jarrett (2000) Determination of hydrologic pathways during snowmelt for alpine/subalpine basins, Rocky Mountain National Park, Colorado WATER RESOURCES RESEARCH, 36: 63–75.

Tague CL, LE Band (2004) RHESSys: Regional Hydro-Ecologic Simulation System—An Object-Oriented Approach to Spatially Distributed Modeling of Carbon, Water, and Nutrient Cycling. Earth Interactions: 8:1-42

USACE (1998) Engineering and Design: RUNOFF FROM SNOWMELT. Manual EM 1110-2-1406. 142p. U.S. Army Corps of Engineers. <http://www.usace.army.mil/publications/eng-manuals/em1110-2-1406/toc.htm>

